acetyl-β-methylcholine bromide (methacholine) were obtained from Sigma (St Louis, MO). Antibodies against HDAC2, IκB-α, the Ser536-phosphorylated form of NF-κB and actin, along with apocynin were from Santa Cruz Biotechnology (Santa Cruz, CA). GeneChip Mouse Gene 1.0 ST Array was from Affymetrix (Santa Clara, CA). Alexa Fluor 594 goat anti-rabbit (or anti-mouse) immunoglobulin G was purchased from Invitrogen (Carlsbad, CA). Antibody against SOD1, gallamine triethiodide and 1,1-dimethyl-4-diphenylacetoxypiperidinium iodide and the HDAC assay kit were from Enzo Life Sciences (Farmingdale, NY). An antibody against 8-OHdG was from Nikken SEIL (Shizuoka, Japan). The GST assay kit was from PromoCell GmbH (Heidelberg, Germany). TransAM Nrf2 kit was from Active Motif (Carlsbad, CA). The SOD assay kit and the nuclear extraction hypotonic buffer were from Cayman Chemical (Ann Arbor, MI). Mounting medium for immunohistochemical analysis (VECTASHIELD) was from Vector Laboratories (Burlingame, CA). Novo-Heparin for injection was from Mochida Pharmaceutical (Tokyo, Japan). Chloral hydrate was from Nacalai Tesque (Kyoto, Japan). Diff-Quik was from the Sysmex Corporation (Kobe, Japan). ELISA kits for tumour necrosis factor-α, macrophage inflammatory protein-2, monocyte chemoattractant protein-1 and keratinocyte-derived chemokine were from R&D Systems (Minneapolis, MN). The RNeasy kit was obtained from Qiagen (Valencia, CA), the PrimeScript 1st strand cDNA Synthesis Kit was from TAKARA Bio (Ohtsu, Japan), and the SsoFast EvaGreen Supermix was from Bio-Rad (Hercules, CA). Pirenzepine dihydrochloride (pirenzepine) and formalin neutral buffer solution were from WAKO Pure Chemicals (Tokyo, Japan). Mayer's hematoxylin, 1% eosin alcohol solution and malinol were from MUTO Pure Chemicals (Tokyo, Japan). DAPI, diethylenetriamine-*N, N, N′, N′, N″*-pentaacetic acid and DPhPMPO were from Dojindo (Kumamoto, Japan). RAW264 cells (a macrophage cell line) were from RIKEN BioResource Center (Tsukuba, Japan). ICR mice (4–6 weeks old, male) and DBA/2 mice (5 weeks old, female) were purchased from Charles River (Yokohama, Japan) and used in all experiments in this paper. The experiments and procedures described here were carried out in accordance with the Guide for the Care and Use of Laboratory Animals as adopted and promulgated by the National Institutes of Health, and were approved by the Animal Care Committee of Keio University and Kumamoto University.

Preparation of BALF and CSE and cell culture. BALF was collected by cannulating the trachea and lavaging the lung with 1 ml of sterile PBS containing 50 units ml^{-1} heparin (two times). About 1.8 ml of BALF was routinely recovered from each animal. The total cell number was counted using a hemocytometer. Cells were stained with Diff-Quik reagents after centrifugation with Cytospin4 (Thermo Electron Corporation, Waltham, MA), and the ratio of neutrophils to total cell number was determined.

Cells from BALF or RAW264 cells were cultured in Eagle's minimal essential medium supplemented with 10% FBS or Eagle's minimal essential medium supplemented with 10% FBS and 0.1 mM non-essential amino acid (Lonza, Allendale, NJ), respectively, in a humidified atmosphere of 95% air with 5% CO_2 at 37 °C.

One cigarette (Peace; Japan Tobacco, Tokyo, Japan) was puffed 15 times over a 5 min period to obtain the smoke, which was bubbled into 5 ml of the culture medium using a 50-ml plastic syringe. The resulting suspension was defined 100% CSE[25].

Analyses of cytokines and chemokines and enzyme activities. Cytokine and chemokine levels were measured by ELISA according to the manufacturer's protocol. The activities of HDAC, SOD, GST and Nrf2 were measured by employing each assay kit according to the manufacturer's protocol. For the measurement of Nrf2 activity, nuclear extract was prepared as described in the manufacturer's protocol.

Measurement of level of superoxide anions. The level of superoxide anions was determined by ESR spin trapping with DPhPMPO[32,33]. Cells collected from BALF were incubated with 0.9% NaCl containing 500 μM diethylenetriamine-*N, N, N′, N′, N″*-pentaacetic acid and 10 mM DPhPMPO for 10 min at 37 °C. ESR spectra were recorded at room temperature on a JES-TE200 ESR spectrometer (JEOL, Tokyo, Japan) under the following conditions: modulation frequency, 100 kHz; microwave frequency, 9.43 GHz; microwave power, 40 mW; scanning field, 330.2–340.2 mT; sweep time, 2 min; field modulation width, 0.25 mT; receiver gain, 400; and time count, 0.3 s. Every buffer and solution used in the reaction mixture used for ESR measurement was treated with Chelex 100 resin (Bio-Rad, Hercules, CA) before use to remove metal cations.

The ESR spectrum was consistent with a previously reported DPhPMPO-OOH spectrum (a hyperfine coupling constant of $a^N = 1.24$ mT, $a_\beta^H = 1.16$ mT, $a^P = 3.95$ mT)[34].

Measurement of NADPH oxidase activity. Cells in BALF were prepared as described above. NADPH oxidase activity in the cells was measured by using lucigenin as a substrate (chemiluminescence)[35]. Samples were incubated with 0.1 mM NADPH in 50 mM phosphate buffer containing 1 mM EGTA, 150 mM sucrose and 0.5 mM lucigenin, and lucigenin chemiluminescence was recorded for 15 min in a microplate reader (MicroLumat Plus LB96V, Berthold Technologies, Bad Wildbad, Germany or Infinite M1000, TECAN Group, Mannedorf, Switzerland).

Histological and immunohistochemical analyses. Lung tissue samples were fixed in 10% formalin neutral buffer solution for 24 h at a pressure of 25 cmH_2O, and then embedded in paraffin before being cut into 4 μm-thick sections.

For histological examination, sections were stained first with Mayer's hematoxylin and then with 1% eosin alcohol solution (H&E staining). Samples were mounted with malinol and inspected with the aid of an Olympus BX51 microscope (Tokyo, Japan).

To determine the MLI (an indicator of airspace enlargement), 20 lines (500 μm) were drawn randomly on the image of section stained with H&E and the intersection points with the alveolar walls were counted to determine the MLI. The morphometric analysis at the light microscopic level was conducted by an investigator blinded to the study protocol.

For immunohistochemical analysis, sections were treated with 20 μg ml^{-1} protease K for antigen activation. Sections were blocked with 2.5% goat serum for 10 min, incubated for 12 h with an antibody against the Ser536-phosphorylated form of NF-κB (1:100 dilution) or 8-OHdG (1:100 dilution) in the presence of 2.5% bovine serum albumin, and then incubated for 2 h with Alexa Fluor 594 goat anti-rabbit (or anti-mouse) immunoglobulin G (1:500 dilution) and DAPI (5 μg ml^{-1}). Samples were mounted with VECTASHIELD and inspected with the aid of a fluorescence microscope (Olympus BX51).

Immunoblotting analysis. Lung homogenates were prepared by homogenization in the buffer (50 mM Tris-HCl pH7.6, 150 mM NaCl, 1% NP-40, 1% sodium deoxycholate and 0.1% SDS) and the protein concentration of the samples was determined by the Bradford reagent[36]. Samples were applied to polyacrylamide SDS gels, subjected to electrophoresis and the resultant proteins immunoblotted with their respective antibodies. Full gel scans were shown in Supplementary Fig. S9.

Real-time RT–PCR analysis. Total RNA was extracted from lung tissues using an RNeasy kit according to the manufacturer's protocol. Samples (2.5 μg RNA) were reverse transcribed using a first-strand cDNA synthesis kit. Synthesized cDNA was used in real-time RT–PCR (Chromo 4 instrument (Bio-Rad, Hercules, CA) experiments using SsoFast EvaGreen Supermix, and analysed with Opticon Monitor Software. Specificity was confirmed by electrophoretic analysis of the reaction products and by inclusion of template- or reverse transcriptase-free controls. To normalize the amount of total RNA present in each reaction, glyceraldehyde-3-phosphate dehydrogenase or hypoxanthine guanine phosphoribosyltransferase cDNA was used as an internal standard.

Primers were designed using the Primer3 or Primer-BLAST website. The primers sequence was shown in Supplementary Table S2.

Treatment of mice with PPE and CS. ICR mice maintained under anaesthesia with chloral hydrate (500 mg kg^{-1}) were given one intratracheal injection of PPE (100 μg per mouse or 15 U kg^{-1}) in PBS *via* micropipette.

DBA/2 or ICR mice were exposed to CS by placing 10–20 mice in a chamber (volume, 45 l) connected to a CS-producing apparatus. Commercial non-filtered cigarettes (Peace; Japan Tobacco, Tokyo, Japan) that yielded 28 mg tar and 2.3 mg nicotine on a standard smoking regimen were used. Mice were exposed to the smoke of 1 cigarette for 35 min, 3 times per day, 5 days per week (from Monday to Friday) for 6 months, or to the smoke of 2 cigarettes for 25 min, 3 times per day for 3 days. The apparatus was configured such that each cigarette was puffed 15 times over a 5-min period.

For the administration of mepenzolate by inhalation, 5–8 mice were placed in a chamber (volume, 45 l) and an ultrasonic nebulizer (NE-U07, Omron, Tokyo, Japan) connected to the chamber was used to nebulize over a 30-min period the entire volume of a solution containing mepenzolate dissolved in 10 ml PBS. For control mice, PBS alone was nebulized. Mice were kept in the chamber for a further 10 min after completion of the nebulization.

For the intratracheal administration of candidate drugs, mice were maintained under anaesthesia with chloral hydrate (500 mg kg^{-1}) and each drug in PBS was administered *via* micropipette. For control mice, PBS alone was administered by the same procedure.

Unless otherwise noted, the first administration of each drug was performed 1 h prior to the PPE administration or 2 h before the CS treatment.

Analyses of lung mechanics and respiratory functions. Measurement of lung mechanics and airway resistance was performed with a computer-controlled small-animal ventilator (FlexiVent, SCIREQ, Montreal, Canada)[32,33]. Mice were anesthetized with chloral hydrate (500 mg kg^{-1}), a tracheotomy was performed, and an 8-mm section of metallic tube was inserted into the trachea. Mice were mechanically ventilated at a rate of 150 breaths per min, using a tidal volume of 8.7 ml kg^{-1} and a positive end-expiratory pressure of 2–3 cmH_2O.

Total respiratory system elastance and tissue elastance were measured by the snap shot and forced oscillation techniques, respectively. All data were analysed using FlexiVent software (version 5.3; SCIREQ, Montreal, Canada).

For measurement of the methacholine-induced increase in airway resistance, mice were exposed to nebulized methacholine (1 mg ml^{-1}) five times for 20 s with a 40-s interval between each and airway resistance was measured after each

methacholine challenge by the snap shot technique. All data were analysed using the FlexiVent software.

Determination of the FEV0.05/FVC ratio was performed with the same computer-controlled small-animal ventilator connected to a negative pressure reservoir (SCIREQ, Montreal, Canada)[32,33]. Mice were tracheotomized and ventilated as described above. The lungs were inflated to a pressure of 30 cm H_2O over 1 s and held at this pressure. After 0.2 s, the pinch valve (connected to ventilator) was closed and after 0.3 s, the shutter valve (connected to negative pressure reservoir) was opened for exposure of the lung to the negative pressure. The negative pressure was held for 1.5 s to ensure complete expiration. FEV0.05/FVC was determined using the FlexiVent software.

Gene expression analysis using DNA microarray. Using 100 ng of total RNA extracted from lung tissues, hybridization and signal detection of GeneChip Mouse Gene 1.0 ST Arrays (Affymetrix, Santa Clara, CA) were performed following the manufacturer's instructions. Gene expression analysis was performed in duplicate for each experimental condition. The raw data were normalized by the robust multi-array average method[37] using the 'affy' package from BioConductor (http://www.bioconductor.org/) and R statistical software version 2.12.1 (http://www.r-project.org/).

For functional analysis, we used Gene Set Enrichment Analysis version 2.0.13 with MSigDB gene sets version 4.0 (ref. 38). A gene set category c2.cp.kegg based on the KEGG pathway database was used, and a custom gene set (SINGH_NFE2L2_TARGETS from the category c2.cgp) was used for the analysis of Nrf2-related gene sets. We used 'Diff_of_Classes' (the difference of class means to calculate fold change) as a metric for ranking genes. All other parameters were set to the default values, except for 'set_min' (the minimum size of gene set) to 10 for the Nrf2-related gene sets. Gene sets satisfying $P<0.05$ and FDR<0.25 were considered significant.

Statistical analysis. All values are expressed as the mean ± s.e.m. Two-way analysis of variance followed by the Tukey test or the Student's *t*-test for unpaired results was used to evaluate differences between three or more groups or between two groups, respectively. Differences were considered to be significant for values of $P<0.05$.

References

1. Rabe, K. F. *et al.* Global strategy for the diagnosis, management, and prevention of chronic obstructive pulmonary disease: GOLD executive summary. *Am. J. Respir. Crit. Care. Med.* **176,** 532–555 (2007).
2. Barnes, P. J. & Stockley, R. A. COPD: current therapeutic interventions and future approaches. *Eur. Respir. J.* **25,** 1084–1106 (2005).
3. Owen, C. A. Proteinases and oxidants as targets in the treatment of chronic obstructive pulmonary disease. *Proc. Am. Thorac. Soc.* **2,** 373–385 discussion 394-375 (2005).
4. Tashkin, D. P. *et al.* A 4-year trial of tiotropium in chronic obstructive pulmonary disease. *N. Engl. J. Med.* **359,** 1543–1554 (2008).
5. Calverley, P. M. *et al.* Salmeterol and fluticasone propionate and survival in chronic obstructive pulmonary disease. *N. Engl. J. Med.* **356,** 775–789 (2007).
6. Alsaeedi, A., Sin, D. D. & McAlister, F. A. The effects of inhaled corticosteroids in chronic obstructive pulmonary disease: a systematic review of randomized placebo-controlled trials. *Am. J. Med.* **113,** 59–65 (2002).
7. Barnes, P. J., Ito, K. & Adcock, I. M. Corticosteroid resistance in chronic obstructive pulmonary disease: inactivation of histone deacetylase. *Lancet* **363,** 731–733 (2004).
8. Drummond, G. R., Selemidis, S., Griendling, K. K. & Sobey, C. G. Combating oxidative stress in vascular disease: NADPH oxidases as therapeutic targets. *Nat. Rev. Drug. Discov.* **10,** 453–471 (2011).
9. Gosker, H. R. *et al.* Altered antioxidant status in peripheral skeletal muscle of patients with COPD. *Respir. Med.* **99,** 118–125 (2005).
10. Rahman, I. & MacNee, W. Antioxidant pharmacological therapies for COPD. *Curr. Opin. Pharmacol.* **12,** 256–265 (2012).
11. Barnes, P. J. Role of HDAC2 in the pathophysiology of COPD. *Annu. Rev. Physiol.* **71,** 451–464 (2009).
12. Rajendrasozhan, S., Yang, S. R., Edirisinghe, I., Yao, H., Adenuga, D. & Rahman, I. Deacetylases and NF-kappaB in redox regulation of cigarette smoke-induced lung inflammation: epigenetics in pathogenesis of COPD. *Antioxid. Redox. Signal.* **10,** 799–811 (2008).
13. Rahman, I. & Adcock, I. M. Oxidative stress and redox regulation of lung inflammation in COPD. *Eur. Respir. J.* **28,** 219–242 (2006).
14. Yao, H. *et al.* Redox regulation of lung inflammation: role of NADPH oxidase and NF-kappaB signalling. *Biochem. Soc. Trans.* **35,** 1151–1155 (2007).
15. Yang, S. R. *et al.* Cigarette smoke induces proinflammatory cytokine release by activation of NF-kappaB and posttranslational modifications of histone deacetylase in macrophages. *Am. J. Physiol. Lung. Cell Mol. Physiol.* **291,** L46–L57 (2006).
16. Wu, C. Chromatin remodeling and the control of gene expression. *J. Biol. Chem.* **272,** 28171–28174 (1997).
17. Ito, K. *et al.* Decreased histone deacetylase activity in chronic obstructive pulmonary disease. *N. Engl. J. Med.* **352,** 1967–1976 (2005).
18. Di Stefano, A. *et al.* Increased expression of nuclear factor-kappaB in bronchial biopsies from smokers and patients with COPD. *Eur. Respir. J.* **20,** 556–563 (2002).
19. Ito, K. *et al.* Histone deacetylase 2-mediated deacetylation of the glucocorticoid receptor enables NF-kappaB suppression. *J. Exp. Med.* **203,** 7–13 (2006).
20. Chen, J. Y. Antispasmodic activity of JB-340 (N-methyl-3-piperidyl-diphenylglycolate methobromide) with special reference to its relative selective action on the sphincter of Oddi, colon and urinary bladder of the dog. *Arch. Int. Pharmacodyn. Ther.* **121,** 78–84 (1959).
21. Buckley, J. P., De, F. J. & Reif, E. C. The comparative antispasmodic activity of N-methyl-3-piperidyl diphenylglycolate methobromide (JB-340) and atropine sulfate. *J. Am. Pharm. Assoc. Am. Pharm. Assoc. (Baltim.)* **46,** 592–594 (1957).
22. Long, J. P. & Keasling, H. H. The comparative anticholinergic activity of a series of derivatives of 3-hydroxy piperidine. *J. Am. Pharm. Assoc. Am. Pharm. Assoc. (Baltim.)* **43,** 616–619 (1954).
23. Tanaka, K. I., Sato, K., Aoshiba, K., Azuma, A. & Mizushima, T. Superiority of PC-SOD to other anti-COPD drugs for elastase-induced emphysema and alteration in lung mechanics and respiratory function in mice. *Am. J. Physiol. Lung. Cell Mol. Physiol.* **302,** L1250–L1261 (2012).
24. Hanania, N. A. & Donohue, J. F. Pharmacologic interventions in chronic obstructive pulmonary disease: bronchodilators. *Proc. Am. Thorac. Soc.* **4,** 526–534 (2007).
25. Suzuki, M. *et al.* Down-regulated NF-E2-related factor 2 in pulmonary macrophages of aged smokers and patients with chronic obstructive pulmonary disease. *Am. J. Respir. Cell Mol. Biol.* **39,** 673–682 (2008).
26. Kundu, J. K. & Surh, Y. J. Nrf2-Keap1 signaling as a potential target for chemoprevention of inflammation-associated carcinogenesis. *Pharm. Res.* **27,** 999–1013 (2010).
27. Mizushima, T. Drug discovery and development focusing on existing medicines: drug re-profiling strategy. *J. Biochem.* **149,** 499–505 (2011).
28. Belmonte, K. E. Cholinergic pathways in the lungs and anticholinergic therapy for chronic obstructive pulmonary disease. *Proc. Am. Thorac. Soc.* **2,** 297–304 discussion 311-292 (2005).
29. Xue, H., Su, J., Sun, K., Xie, W. & Wang, H. Glutathione S-transferase M1 and T1 gene polymorphism and COPD risk in smokers: an updated analysis. *Mol. Biol. Rep.* **39,** 5033–5042 (2012).
30. Gross, N. J., Giembycz, M. A. & Rennard, S. I. Treatment of chronic obstructive pulmonary disease with roflumilast, a new phosphodiesterase 4 inhibitor. *COPD* **7,** 141–153 (2010).
31. Miravitlles, M. & Anzueto, A. Insights into interventions in managing COPD patients: lessons from the TORCH and UPLIFT studies. *Int. J. Chron. Obstruct. Pulmon. Dis.* **4,** 185–201 (2009).
32. Tanaka, K., Sato, K., Aoshiba, K., Azuma, A. & Mizushima, T. Superiority of PC-SOD to other anti-COPD drugs for elastase-induced emphysema and alteration in lung mechanics and respiratory function in mice. *Am. J. Physiol. Lung. Cell Mol. Physiol.* **302,** L1250–L1261 (2012).
33. Tanaka, K. *et al.* Therapeutic effect of lecithinized superoxide dismutase on pulmonary emphysema. *J. Pharmacol. Exp. Ther.* **338,** 810–818 (2011).
34. Karakawa, T. *et al.* Applicability of new spin trap agent, 2-diphenylphosphinoyl-2-methyl-3,4-dihydro-2H-pyrrole N-oxide, in biological system. *Biochem. Biophys. Res. Commun.* **370,** 93–97 (2008).
35. Griendling, K. K., Minieri, C. A., Ollerenshaw, J. D. & Alexander, R. W. Angiotensin II stimulates NADH and NADPH oxidase activity in cultured vascular smooth muscle cells. *Circ. Res.* **74,** 1141–1148 (1994).
36. Bradford, M. M. A rapid and sensitive method for the quantitation of microgram quantities of protein utilizing the principle of protein-dye binding. *Anal. Biochem.* **72,** 248–254 (1976).
37. Irizarry, R. *et al.* Exploration, normalization, and summaries of high density oligonucleotide array probe level data. *Biostatistics.* **4,** 249–264 (2003).
38. Subramanian, A. *et al.* Gene set enrichment analysis: a knowledge-based approach for interpreting genome-wide expression profiles. *Proc. Natl Acad. Sci. USA* **102,** 15545–15550 (2005).

Acknowledgements

We thank Dr. Tomoko Betsuyaku (Keio University) for critical reading of this manuscript and Mrs. Kumi Matsuura, Mrs. Arisa Oyama and Mr. Yuri Miyazaki (Kumamoto University) for technical assistance. This work was supported by Grants-in-Aid for Scientific Research from the Ministry of Health, Labour, and Welfare of Japan, as well as the Japan Science and Technology Agency and Grants-in-Aid for Scientific Research from the Ministry of Education, Culture, Sports, Science and Technology, Japan.

Author contributions

Conception and design: K.-I.T., T.M.; analysis and interpretation: K.-I.T., T.I., T.S., D.K., Y.Y., K.I., K.M., K.S.; drafting the manuscript for important intellectual content: K.-I.T., T.I., N.Y., K.-I.T., K.M., H.T., K.S., H.S., T.M.

Additional information

Supplementary Information accompanies this paper at http://www.nature.com/naturecommunications

Competing financial interests: The authors declare no competing financial interests.

Reprints and permission information is available online at http://npg.nature.com/reprintsandpermissions/

How to cite this article: Tanaka, K.-I. *et al.* Mepenzolate bromide displays beneficial effects in a mouse model of chronic obstructive pulmonary disease. *Nat. Commun.* 4:2686 doi: 10.1038/ncomms3686 (2013).

Bioorganic & Medicinal Chemistry 22 (2014) 2529–2534

Contents lists available at ScienceDirect

Bioorganic & Medicinal Chemistry

journal homepage: www.elsevier.com/locate/bmc

Structure–activity relationship of celecoxib and rofecoxib for the membrane permeabilizing activity

Naoki Yamakawa [a,b,†], Koichiro Suzuki [a,†], Yasunobu Yamashita [a], Takashi Katsu [c], Kengo Hanaya [a], Mitsuru Shoji [a], Takeshi Sugai [a], Tohru Mizushima [a,*]

[a] Faculty of Pharmacy, Keio University, Tokyo 105-8512, Japan
[b] Shujitsu University School of Pharmacy, Okayama 703-8516, Japan
[c] Graduate School of Medicine, Dentistry and Pharmaceutical Sciences, Okayama University, Okayama 700-8530, Japan

ARTICLE INFO

Article history:
Received 21 January 2014
Revised 19 February 2014
Accepted 22 February 2014
Available online 12 March 2014

Keywords:
Celecoxib
Rofecoxib
COX-2 selectivity
Membrane permeabilization
Gastric adverse effect

ABSTRACT

Non-steroidal anti-inflammatory drugs (NSAIDs) achieve their anti-inflammatory effect by inhibiting cyclooxygenase activity. We previously suggested that in addition to cyclooxygenase-inhibition at the gastric mucosa, NSAID-induced gastric mucosal cell death is required for the formation of NSAID-induced gastric lesions in vivo. We showed that celecoxib exhibited the most potent membrane permeabilizing activity among the NSAIDs tested. In contrast, we have found that the NSAID rofecoxib has very weak membrane permeabilizing activity. To understand the membrane permeabilizing activity of coxibs in terms of their structure–activity relationship, we separated the structures of celecoxib and rofecoxib into three parts, synthesized hybrid compounds by substitution of each of the parts, and examined the membrane permeabilizing activities of these hybrids. The results suggest that the sulfonamidophenyl subgroup of celecoxib or the methanesulfonylphenyl subgroup of rofecoxib is important for their potent or weak membrane permeabilizing activity, respectively. These findings provide important information for design and synthesis of new coxibs with lower membrane permeabilizing activity.

1. Introduction

Non-steroidal anti-inflammatory drugs (NSAIDs) are one of the most frequently used classes of medicines.[1] NSAIDs are inhibitors of cyclooxygenase (COX), a protein essential for the synthesis of prostaglandins (PGs), which have a strong ability to induce inflammation. However, NSAID use is associated with gastrointestinal complications, such as gastric ulcers and bleeding. In the United States, about 16,500 people per year die as a result of NSAID-associated gastrointestinal complications.[2] Thus, understanding the mechanism of NSAID-induced gastric lesions and its application to design and synthesis of new NSAIDs with reduced adverse effects on the gastric mucosa is important.

The inhibition of COX by NSAIDs was initially thought to be responsible for the adverse gastric side effects manifested by such treatment, because PGs have a strong protective effect on the gastric mucosa. Thus, after the identification of two subtypes of COX (COX-1 and COX-2), which are responsible for the majority of COX activity at the gastric mucosa and in inflammatory tissues, respectively,[3,4] selective COX-2 inhibitors (most of which are coxibs, such as celecoxib and rofecoxib) were developed as NSAIDs with reduced adverse gastric side effects.[5–7] However, due to the observation that rofecoxib was associated with an increased potential risk of cardiovascular thrombotic events,[8,9] this NSAID was withdrawn from the market. At first, this increased risk was believed to be due to the class effect of selective COX-2 inhibitors, because prostacyclin, a potent anti-aggregator of platelets and a vasodilator, is mainly produced by COX-2.[10–12] However, some clinical studies showed that the potential risk of cardiovascular thrombotic events was indistinguishable between celecoxib users and classic NSAID users.[13,14] Thus, it is possible that the increased potential risk of cardiovascular thrombotic events is not due to the class effect of selective COX-2 inhibitors, but rather is a specific characteristic of rofecoxib. While mechanisms to explain this rofecoxib-specific increase in the potential risk of cardiovascular thrombotic events have been proposed,[15–17] a definitive explanation for this increase has not yet been forthcoming.

It is now believed that the inhibition of COX by NSAIDs is not the sole explanation for the adverse gastric side effects of NSAIDs, given that the increased incidence of gastric lesions and the

* Corresponding author. Tel.: +81 354002628.
E-mail address: mizushima-th@pha.keio.ac.jp (T. Mizushima).
† These two authors contributed to this paper equally.

http://dx.doi.org/10.1016/j.bmc.2014.02.032
0968-0896/

decrease in PG levels induced by NSAIDs do not always occur in parallel.[18–20] We proposed that, in addition to COX-inhibition at the gastric mucosa, NSAID-induced gastric mucosal cell death is required for the formation of NSAID-induced gastric lesions in vivo.[21,22] Furthermore, we reproduced NSAID-induce cell death in cultured gastric mucosal cells in vitro[22–26] and showed that the primary target of NSAIDs for the induction of cell death is the cytoplasmic membrane. Moreover, a close relationship between membrane permeabilizing activity and cell death-inducing activity among various NSAIDs was shown.[23,25] Thus, decreasing the membrane permeabilizing activity of NSAIDs may be another strategy to synthesize safer NSAIDs for the gastric mucosa. In fact, we recently reported that screening for NSAIDs with lower membrane permeabilizing activity resulted in the identification of an interesting new NSAID, fluoro-loxoprofen, which has much lower membrane permeabilizing and gastric ulcerogenic activities compared with clinically used NSAIDs.[27–31] These results suggest that NSAIDs with lower membrane permeabilizing activity could be therapeutically beneficial. Thus, it is important to understand how the membrane permeabilizing properties of NSAIDs are affected by their structure–activity relationship.

We previously reported that celecoxib showed the most potent membrane permeabilizing and cytotoxic activities among the NSAIDs we tested.[23,25] We also reported that the cytotoxic activity of rofecoxib is much lower than that of celecoxib.[21] As these results suggested that the membrane permeabilizing activity of rofecoxib is lower than that of celecoxib, our objective here was to confirm this hypothesis.

Furthermore, to identify how the structure–activity relationship of coxibs affects their membrane permeabilizing activity, we synthesized hybrid compounds from celecoxib and rofecoxib and examined their membrane permeabilizing activities. The results suggest that the sulfonamidophenyl subgroup of celecoxib and the methanesulfonylphenyl subgroup of rofecoxib are important for determining the membrane permeabilizing activities of these NSAIDs.

2. Chemistry

The synthetic route for target compounds **3–5** is outlined in Scheme 1. Pyrazole compounds **3–5** were synthesized by the condensation of appropriate 1,3-diketones and hydrazine. The reaction of 4,4,4-trifluoro-1-*p*-tolylbutane-1,3-dione **9** with 4-methylphenylhydrazine hydrochloride **11**, 4,4,4-trifluoro-1-phenylbutane-1,3-dione **10** with **11**, or **10** with 4-sulfamoylphenylhydrazine hydrochloride **12** afforded target compounds **3**, **4** or **5**, respectively.

The synthetic route for target compounds **6–8** is outlined in Scheme 2. Furanone compounds **6–8** were synthesized by the condensation of a phenylacetic acid analog and phenacyl bromide. The reaction of **13** with **15**, **14** with **17** or **14** with **16** in the presence of triethylamine afforded the phenacyl phenylacetate products **18**, **19** or **20**, respectively. Treatment of intermediates **18–20** with 1,8-diazabicyclo[5.4.0]undec-7-ene (DBU) provided 3,4-diphenyl-2(5*H*)furanone **21** or target compounds **7** or **8**. chlorosulfonylation of **21** by the reaction with chlorosulfonic acid followed by sulfonamidation using ammonium hydroxide gave target compound **6**.

The final compounds were characterized by nuclear magnetic resonance (NMR), infrared spectroscopy (IR), high resolution mass spectra (HR-MS) and elemental analysis.

3. Results and discussion

The chemical structures of celecoxib and rofecoxib exhibit some similarities (Fig. 1) and can be divided into three parts (A–C in Table 1); part A, methylphenyl for celecoxib, phenyl for rofecoxib; part B, trifluoromethylpyrazole for celecoxib, furanone for rofecoxib; part C, sulfonamidophenyl for celecoxib, methanesulfonylphenyl for rofecoxib. Thus, in addition to celecoxib and rofecoxib, there are six possible combinations of these three parts that could be used to obtain hybrid compounds of celecoxib and rofecoxib (compounds **3–8** in Table 1). We synthesized these six compounds and tested their membrane permeabilizing and COX-inhibitory activities.

To begin with, we used calcein-loaded liposomes to compare the membrane permeabilizing activities of celecoxib and rofecoxib. As calcein fluorescence is very weak at high concentrations due to self-quenching, the addition of membrane-permeabilizing drugs to a medium containing calcein-loaded liposomes causes an increase in fluorescence by diluting the calcein.[25] As shown in Figure 2, celecoxib and rofecoxib increased the calcein fluorescence in a dose-dependent manner. Compared with celecoxib, however, a rofecoxib concentration about 100 times higher was required to increase the fluorescence by the same amount. Figure 2 shows that rofecoxib has a much lower membrane permeabilizing activity than celecoxib.

We next examined the membrane permeabilizing activities of the six hybrid compounds in a similar manner. As shown in Figure 3, all of the hybrid compounds increased the calcein fluorescence in a dose-dependent manner. To compare the membrane permeabilizing activity of these compounds, we used the EC_{50} (half-maximal effective concentration) index, which is defined as the concentration of each compound required for 50% of the calcein in loaded liposomes to be released (Table 2). Comparison of the EC_{50} index of **3**, **5** and **8** (compounds with one part substitution from celecoxib) showed that the membrane permeabilizing activity of **3** was much lower than that of **5** or **8**, suggesting that part

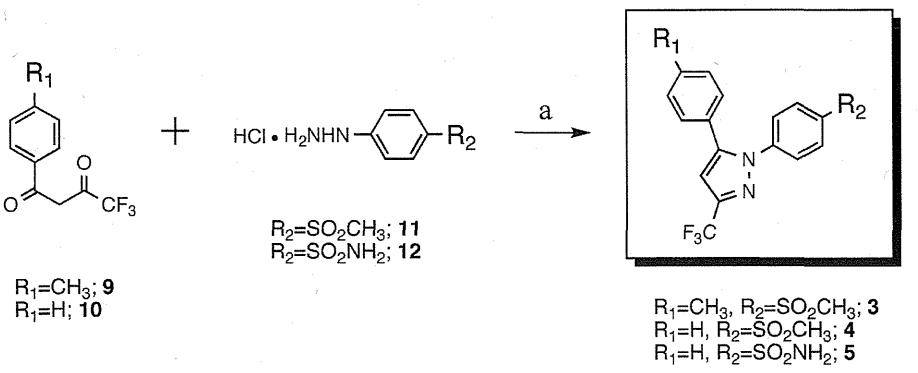

Scheme 1. Synthesis of pyrazole compounds **3–5**.

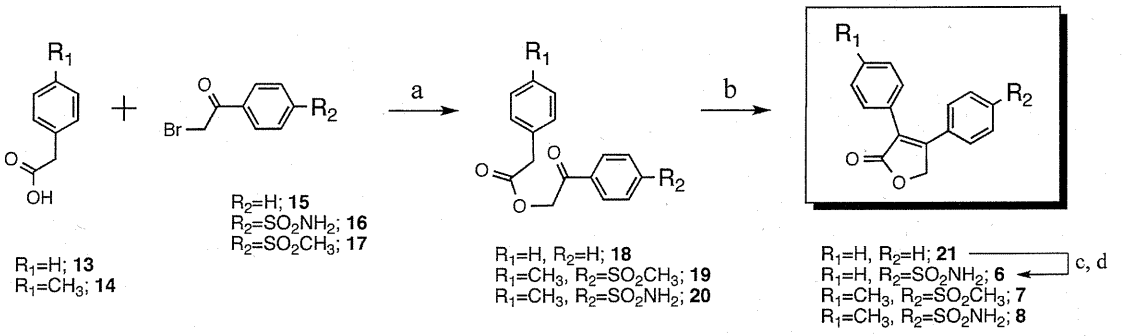

Scheme 2. Synthesis of furanone compounds **6–8**.

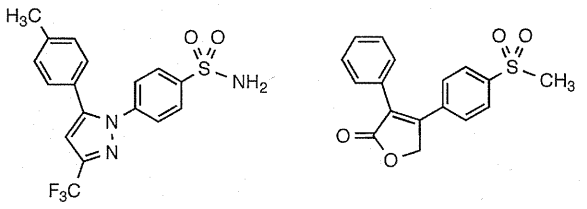

Figure 1. Structures of celecoxib and rofecoxib.

C of celecoxib (the sulfonamidophenyl subgroup) is the most important subgroup determining its high membrane permeabilizing activity. On the other hand, comparison of the EC_{50} index of **4**, **6** and **7** (compounds with one part substitution from rofecoxib) revealed that the membrane permeabilizing activity of **6** was higher than that of **4** or **7**. In this case, part C of rofecoxib (the methanesulfonylphenyl subgroup) was also seemed to be the most important subgroup determining its low membrane permeabilizing activity. Thus, part C seems to be important for determining the permeabilizing activity of these coxibs. The fundamental structural requirement underlying the ability of molecule to permeabilize membrane is a shape in which clusters of hydrophobic and hydrophilic parts are spatially organized with appropriate distance, because this structure enable the hydrophobic part to be located near the surface of membrane, resulting in perturbation of membrane structure. In the present case, because the sulfonamidophenyl subgroup is more hydrophilic than the methanesulfonylphenyl subgroup, the former but not the latter produces hydrophilic part. The methanesulfonylphenyl subgroup is hydrophobic enough to be totally buried within the lipid bilayer structure and therefore, does not affect the membrane structure drastically. On the other hand, the sulfonamidophenyl subgroup is relatively hydrophilic, which allows the compound to face membrane surface, resulting in perturbation of the membrane structure.

Table 1
Structures of celecoxib, rofecoxib and their hybrid compounds (**3–8**)

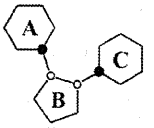

	A	B	C		A	B	C
Celecoxib	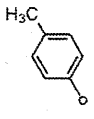	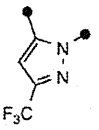	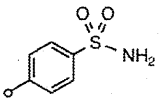	Rofecoxib		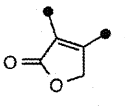	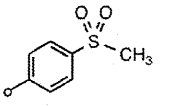
3	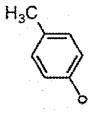	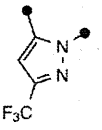	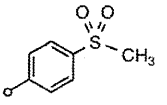	**6**		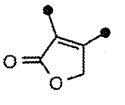	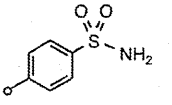
4	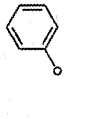	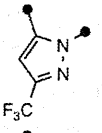	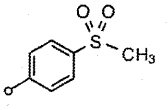	**7**	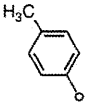	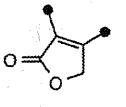	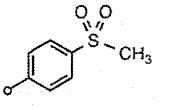
5	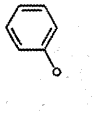	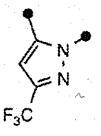	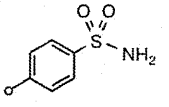	**8**		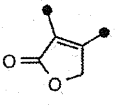	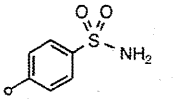

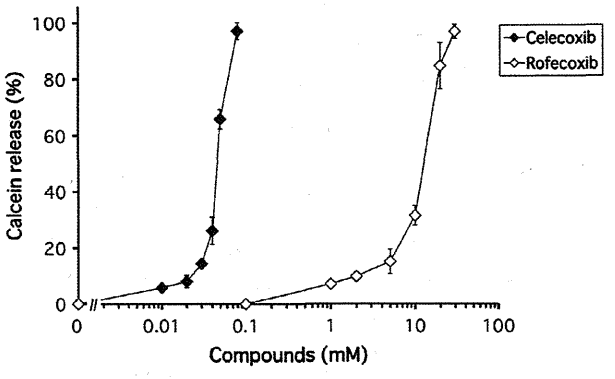

Figure 2. Membrane permeabilization by celecoxib and rofecoxib. Calcein-loaded liposomes were incubated for 10 min at 30 °C with the indicated concentration of each compound. The release of calcein from the liposomes was determined by measuring fluorescence intensity as described in the experimental section. Triton X-100 (10 μM) was used to establish the 100% level of calcein release. Values are mean ± SD ($n = 3$).

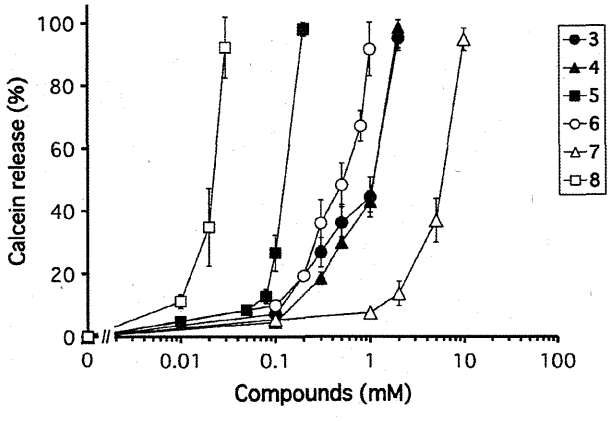

Figure 3. Membrane permeabilization by pyrazole compounds **3–5** and furanone compounds **6–8**. Experiments and data analysis were performed as described in the legend of Fig. 2. Values shown are mean ± SD ($n = 3$).

The results presented in Figures 2 and 3 thus provide important information for the design and synthesis of new coxibs with lower membrane permeabilizing activity.

The ionization of these compounds would not be related to their membrane permeabilizing activities. This is because pK_a values of all compounds (celecoxib, rofecoxib, **3**– **8**) are higher than 10 and membrane permeabilizing assay was performed under the conditions of pH = 6.8. Furthermore, such ionization would increase the osmotic pressure outside vesicles and thus, would not stimulate the release of calcein from vesicles.

The inhibitory effects on COX-1 and COX-2 of these compounds were compared by using the IC_{50} (half-maximal inhibitory concentration) index, which is defined as the concentration of each compound required for 50% inhibition of each enzyme. The IC_{50} values for COX-1 and COX-2 of celecoxib and rofecoxib were roughly similar to those reported previously,[32] and the IC_{50} values for COX-1 of all the hybrid compounds were relatively high (Table 2). With the exception of **4** and **6**, the IC_{50} values for COX-2 of the hybrid compounds were within the range seen for celecoxib and rofecoxib, and all the hybrid compounds (except 6) showed COX-2 selectivity (Table 2). Since both **4** and **6** are compounds with one part substitution from rofecoxib, the structure of rofecoxib rather than that of celecoxib appears to be sensitive to modification in relation to COX-2 inhibitory activity.

Table 2
Membrane permeabilizing activities and inhibitory activities on COX-1 and COX-2 of celecoxib, rofecoxib and their hybrid compounds (**3–8**)

Compounds	EC_{50} (mM)	IC_{50} (μM)		COX-1/COX-2	EC_{50}/IC_{50}
	Calcein release	COX-1	COX-2		
Celecoxib	0.050	117	0.07	1670	0.71
Rofecoxib	12.6	>500	0.36	>1380	35.0
3	1.44	>500	0.13	>3830	11.1
4	1.30	>500	6.84	>73	0.19
5	0.12	213	0.16	1330	0.75
6	0.48	>500	>500	–	–
7	6.23	>500	0.30	>1680	20.8
8	0.024	385	0.11	>3500	0.22

The EC_{50} value for membrane permeabilization (concentration of each compound required for 50% release of calcein) was calculated based on the data shown in Figures 2 and 3. The inhibitory effect of each compound on COX-1 and COX-2 was examined using purified ovine COX-1 and human recombinant COX-2 as described in the experimental section. The values of IC_{50} (concentration of each compound required for 50% inhibition) were estimated from the sigmoid-like dose-response curve (4-parameter logistic curve model) drawn using logistic-curve fitting software (ImageJ 1.43u; National Institutes of Health, USA), and the COX-1/COX-2 ratios of IC_{50} values were calculated. EC_{50} for membrane permeabilization/IC_{50} for COX-2 inhibition was shown. Values are mean ($n = 3$).

Among the six hybrid compounds, **4** and **6** can be eliminated as candidates for future clinical use based on their relatively weak inhibitory activity on COX-2 (Table 2). On the other hand, **5** and **8** can be eliminated as candidates based on their relatively potent membrane permeabilizing activity (Table 2). To further compare the potential value of these compounds, we calculated the value of the EC_{50} index for calcein release/IC_{50} index for COX-2 (Table 2). Compounds **3** and **7** appear as the most likely selections as candidates for future clinical use based on this index (Table 2). As described in the introduction section, rofecoxib was withdrawn from the market due to an observed increased potential risk for cardiovascular thrombotic events,[8,9] which may not be a drug class effect but actually something characteristic of rofecoxib alone. According to this hypothesis, it could be postulated that **3** and **7** might have fewer adverse effects associated with their use. Nevertheless, because the mechanism underlying the increased cardiovascular thrombotic events remains to be elucidated, the potential risk of these compounds has not yet been tested without a large-scale clinical study.

4. Conclusion

We here found that rofecoxib has very weak membrane permeabilizing activity compared with celecoxib. Furthermore, analysis of the membrane permeabilizing activities of hybrid compounds derived from celecoxib and rofecoxib suggested that the sulfonamidophenyl subgroup of celecoxib and the methanesulfonylphenyl subgroup of rofecoxib are important for their potent or weak membrane permeabilizing activity, respectively.

5. Experimental section

5.1. Chemistry

All solvents and reagents were purchased from Tokyo Chemical Industry Co., Ltd (Tokyo, Japan) or Wako Pure Chemical Industries (Tokyo, Japan) and used without further purification. Fourier transform IR spectra were recorded as films with NaCl plates on a JASCO FT/IR-480 spectrophotometer. ^{1}H NMR and ^{13}C NMR spectra were recorded on VARIAN 400- or 500-MR spectrometer (Agilent Thechnologies Japan, Tokyo, Japan) operating at 400 MHz, in a ca. 2% solution of $CDCl_3$ or DMSO-d_6. Coupling constant (J) values are estimated in hertz (Hz) and spin multiples are given as s (singlet), d

(double), m (multiplet), and br (broad). Mass spectra were detected with an electrospray ionization time-of-flight (ESI-TOF) mass spectrometer (Bruker MicroTOF, Bruker, Bremen, Germany) in the negative mode. The progress of all reactions was monitored by thin-layer chromatography (TLC) with silica gel glass plates (60 F_{254}) (Merck Ltd, Tokyo, Japan), and spots were visualized with ultraviolet (UV) light (254 nm) and stained with 5% ethanolic phosphomolybdic acid. Column chromatography was performed using Silica gel 60 N (Kanto Chemical Co., Tokyo, Japan). Elemental analyses were performed for C, H and N (Central Service Research Center, Keio University) and were within ±0.4% of the theoretical values. Melting points (mp) were obtained using a Yanaco melting point apparatus MP-J3 (Yanaco, Kyoto, Japan) without correction. Celecoxib and rofecoxib were from LKT Laboratories Inc. Egg phosphatidylcholine (PC) was from Kanto Chemicals Co. (Tokyo, Japan).

5.1.1. General procedure for preparation of compounds 3–5

Phenylhydrazine hydrochloride (**11** or **12**) was added to a stirred solution of the dione (**9** or **10**) in ethanol (30 mL), and the mixture was refluxed for 20 h. After cooling to room temperature, the reaction mixture was concentrated in vacuo. The resulting residue was dissolved in AcOEt (50 mL) and washed with brine. The organic fraction was dried over Na_2SO_4 and filtered. The filtrate was concentrated in vacuo and the residue was purified by silica gel chromatography (*n*-hexane/AcOEt, 2:1) to afford pyrazole compounds **3–5**.

5.1.2. 1-(4-Methanesulfonylphenyl)-5-*p*-tolyl-3-(trifluoromethyl)-1*H*-pyrazole (3)

Compound **3** was synthesized from **9** (500 mg, 2.2 mmol, 1.0 equiv) and **11** (774 mg, 3.5 mmol, 1.6 equiv). Colorless needle-like crystals (yield 35%); mp 125.1–126.1 °C; IR (film) *v*: 1160, 1325 (SO_2), 2930 (C-H), 3015 (Ar-H) cm^{-1}; ^1H NMR ($CDCl_3$, 500 MHz) *δ*: 2.36 (s, 3H, Ar-CH_3), 3.04 (s, 3H, SO_2CH_3), 6.72 (s, 1H, pyrazole-H4), 7.10 (d, *J* = 8.0, 2H, *p*-tolyl-H3, -H5), 7.16 (d, *J* = 8.0, 2H, *p*-tolyl-H2, -H6), 7.52 (d, *J* = 8.0, 2H, methanesulfonylphenyl-H2, -H6), 7.91 (d, *J* = 8.0, 2H, methanesulfonylphenyl-H3, -H5); HR-ESI-TOF/MS (negative, *m/z*): 379.0706 ($[M-H]^-$, Calcd for $C_{18}H_{14}F_3N_2O_2S$: 379.0728). Anal. Calcd for $C_{18}H_{15}F_3N_2O_2S$: C, 56.84; H, 3.97; N, 7.36. Found: C, 56.64; H, 3.75; N, 7.20. IR and ^1H NMR spectral data for **3** were consistent with reported results.[33,34]

5.1.3. 1-(4-Methanesulfonylphenyl)-5-phenyl-3-(trifluoromethyl)-1*H*-pyrazole (4)

Compound **4** was synthesized from **10** (500 mg, 2.3 mmol, 1.0 equiv) and **11** (567 mg, 2.5 mmol, 1.6 equiv). Colorless needle-like crystals (yield 50%); mp 135.2–136.1 °C; IR (film) *v*: 1162, 1320 (SO_2), 2935 (C-H), 3020 (Ar-H) cm^{-1}; ^1H NMR ($CDCl_3$, 500 MHz) *δ*: 3.04 (s, 3H, SO_2CH_3), 6.77 (s, 1H, pyrazole-H4), 7.22–7.23 (m, 2H, phenyl-H2, -H6), 7.35–7.41 (m, 3H, phenyl-H3, -H4, -H5), 7.51 (d, *J* = 8.5, 2H, methanesulfonylphenyl-H2, -H6), 7.91 (d, *J* = 8.5, 2H, methanesulfonylphenyl-H3, -H5); ^{13}C NMR ($CDCl_3$, 500 MHz) *δ*: 44.28, 106.6, 125.5, 128.4, 128.7, 129.0, 129.5, 139.8, 143.2, 144.0, 144.3, 145.1; HR-ESI-TOF/MS (negative, *m/z*): 365.0550 ($[M-H]^-$, Calcd for $C_{17}H_{12}F_3N_2O_2S$: 365.0572). Anal. Calcd for $C_{17}H_{13}F_3N_2O_2S$: C, 55.73; H, 3.58; N, 7.65. Found: C, 55.58; H, 3.60; N, 7.44.

5.1.3.1. 1-(4-Sulfonamidophenyl)-5-phenyl-3-(trifluoromethyl)-1*H*-pyrazole (5).

Compound **5** was synthesized from **10** (500 mg, 2.3 mmol, 1.0 equiv) and **12** (560 mg, 3.5 mmol, 1.6 equiv). Colorless needle-like crystals (yield 66%); mp 164.1–165.2 °C; IR (film) *v*: 1165, 1325 (SO_2), 3025 (Ar-H), 3680 (N-H) cm^{-1}; ^1H NMR ($CDCl_3$, 400 MHz) *δ*: 4.92 (br s, 2H, NH_2), 6.75 (s, 1H, pyrazole-H4), 7.22–7.24 (m, 2H, phenyl-H2, -H6), 7.32–7.40 (m, 3H, phenyl-H3, -H4, -H5), 7.45 (d, *J* = 8.5, 2H, 4-sulfonamidophenyl-H2, -H6), 7.88 (d, *J* = 8.5, 2H, 4-sulfonamidophenyl-H3, -H5); HR-ESI-TOF/MS (negative, *m/z*): 368.0622 ($[M-H]^-$, Calcd for $C_{16}H_{12}F_3N_2O_2S$: 368.0681). Anal. Calcd for $C_{16}H_{13}F_3N_2O_2S$: C, 52.17; H, 3.56; N, 11.41. Found: C, 52.12; H, 3.45; N, 11.28. ^1H NMR spectral data for **5** were consistent with reported results.[35,36]

5.1.4. General procedure for preparation of compounds 21, 7 and 8

To a stirred solution of phenylacetic acid (**13** or **14**) and triethylamine in dry CH_3CN, phenacyl bromide (**15–17**) in dry CH_3CN was added dropwise at room temperature. The reaction mixture was stirred for 1 h and was concentrated in vacuo. The resulting residue was re-dissolved in AcOEt (50 mL) and washed with 1 M HCl (20 mL). The organic fraction was dried over Na_2SO_4 and filtered. The filtrate was evaporated under reduced pressure to give crude product (**18–20**) that was used in the next step without further purification.

DBU (1.0 equiv) in dry CH_3CN (2 mL) was added dropwise to a stirred solution of the crude intermediate (**18–20**, 1.0 equiv) in dry CH_3CN (8 mL) at 0 °C. After stirring at 0 °C for 15 min, the mixture was poured into dilute HCl solution and the product was extracted with AcOEt. Evaporation of the solvent and purification of the residue by silica gel chromatography (n-hexane/AcOEt, 2:1) yielded the furanone compounds **21**, **7** or **8**.

5.1.4.1. 3-Phenyl-4-(4-sulfonamidophenyl)-2(5*H*)-furanone (6).

Compound **6** was prepared by chlorosulfonylation in chloroform and sulfonamide formation using ammonium hydroxide in ethanol of **21** that was obtained from phenylacetic acid (**13**, 0.5 g, 3.7 mmol, 1.0 equiv) and 4-sulfonamidophenacyl bromide (**15**, 1.03 g, 3.7 mmol, 1.0 equiv) via the intermediate **18** by the method described previously.[36] Colorless needle-like crystals (yield 22%, three steps); mp 248.2–249.5 °C; IR (film) *v*: 1145, 1320 (SO_2), 1740 (C=O), 3030 (Ar-H), 3230 (N-H) cm^{-1}; ^1H NMR (DMSO-d_6, 400 MHz) *δ*: 5.42 (s, 2H, CH_2), 7.35–7.53 (m, 5H, phenyl-H), 7.42 (br s, 2H, NH_2), 7.52 (d, *J* = 8.6, 2H, 4-sulfonamidophenyl-H2, -H6), 7.85 (d, *J* = 8.6, 2H, 4-sulfonamidophenyl-H3, -H5); HR-ESI-TOF/MS (negative, *m/z*): 314.0495 ($[M-H]^-$, Calcd for $C_{16}H_{12}NO_4S$: 314.0487). Anal. Calcd for $C_{16}H_{13}NO_4S$: C, 60.94; H, 4.16; N, 4.44. Found: C, 61.01; H, 4.02; N, 4.30. IR and ^1H NMR spectral data for **6** were consistent with reported results.[37,38]

5.1.4.2. 3-(4-Methylphenyl)-4-(4-methanesulfonylphenyl)-2(5*H*)-furanone (7).

Compound **7** was synthesized via the intermediate **19** from 4-methylphenylacetic acid (**14**, 0.5 g, 3.7 mmol, 1.0 equiv) and 4-methanesulfonylphenacyl bromide (17, 1.03 g, 3.7 mmol, 1.0 equiv). Yellow needle-like crystals (yield 67%, two steps); mp 174.5–175.4 °C; IR (film) *v*: 1150, 1320 (SO_2), 1750 (C=O), 3040 (Ar-H), 2930 (C-H) cm^{-1}; ^1H NMR ($CDCl_3$, 400 MHz) *δ*: 2.38 (s, 3H, Ar-CH_3), 3.07 (s, 3H, SO_2CH_3), 5.17 (s, 2H, CH_2), 7.20 (d, *J* = 8.1, 2H, *p*-tolyl-H3, -H5), 7.28 (d, *J* = 8.2, 2H, *p*-tolyl-H2, -H6), 7.52 (dd, *J* = 6.8, 2.0, 2H, methanesulfonylphenyl-H2, -H6), 7.92 (dd, *J* = 6.8, 2.0, 2H, methanesulfonylphenyl-H3, -H5); HR-ESI-TOF/MS (negative, *m/z*): 327.0718 ($[M-H]^-$, Calcd for $C_{18}H_{15}O_4S$: 327.0691). Anal. Calcd for $C_{18}H_{16}O_4S$: C, 65.84; H, 4.91. Found: C, 66.12; H, 5.00. IR and ^1H NMR spectral data for **7** were consistent with reported results.[39]

5.1.4.3. 3-(4-Methylphenyl)-4-(4-sulfonamidophenyl)-2(5*H*)-furanone (8).

Compound **8** was synthesized via the intermediate **20** from 4-methylphenylacetic acid (14, 0.5 g, 3.7 mmol, 1.0 equiv) and 4-sulfonamidophenacyl bromide (16, 1.03 g, 3.7 mmol, 1.0 equiv). Yellow needle-like crystals (yield 67%, two steps); mp 218.5–219.2 °C; IR (film) *v*: 1140, 1325 (SO_2), 1735 (C=O), 3025 (Ar-H), 3220 (N-H), 2925 (C-H)cm^{-1}; ^1H NMR (DMSO-d_6,

400 MHz) δ: 2.32 (s, 3H, Ar-CH_3), 3.32 (s, 3H, SO_2CH_3), 5.36 (s, 2H, CH_2), 7.22 (d, J = 8.0, 2H, *p*-tolyl-H3, -H5), 7.24 (d, J = 8.0, 2H, *p*-tolyl-H2, -H6), 7.44 (brs, 2H, NH_2), 7.54 (d, J = 8.8, 2H, 4-sulfonamidophenyl-H2, -H6), 7.80 (d, J = 8.8, 2H, 4-sulfonamidophenyl-H3, -H5); HR-ESI-TOF/MS (negative, m/z): 328.0694 ($[M-H]^-$, Calcd for $C_{17}H_{14}NO_4S$: 328.0644). Anal. Calcd for $C_{17}H_{15}NO_4S$: C, 61.99; H, 4.59; N, 4.25. Found: C, 62.05; H, 4.68; N, 4.42.

5.2. Membrane permeability assay

Permeabilization of calcein-loaded liposomes was assayed as described previously,[25] with some modifications. Liposomes were prepared using the reversed-phase evaporation method. Egg phosphatidylcholine (PC) (10 μmol, 7.7 mg) was dissolved in chloroform/methanol (1:2, v/v), dried, dissolved in 1.5 mL of diethyl ether and added to 1 mL of 100 mM calcein-NaOH (pH 7.4). The mixture was then sonicated to obtain a homogenous emulsion. The diethyl ether solvent was removed and the resulting suspension of liposomes was centrifuged and washed twice with fresh buffer A (10 mM phosphate buffer (Na_2HPO_4/NaH_2PO_4) (pH 6.8) containing 150 mM NaCl) to remove untrapped calcein. The final liposome precipitate was re-suspended in 5 mL buffer A. A 30 μL aliquot of this suspension was diluted with buffer A to 20 mL and the diluted suspension was then incubated at 30 °C for 10 min in the presence of each compound. The release of calcein from liposomes was determined by measuring the fluorescence intensity at 520 nm (excitation at 490 nm). The EC_{50} value was estimated from non-linear regression plots with the average of triplicate experiments for each compound; Triton X-100 (10 μM) was used to establish the 100% level of calcein release.

5.3. COX-inhibition assay

The inhibitory effect of each compound on COX-1 and COX-2 activity was examined using an enzyme immunoassay (EIA) kit (Cayman Chemical, Ann Arbor, MI, USA), including purified ovine COX-1 and human recombinant COX-2 according to the manufacturer's procedures.

Acknowledgments

This work was supported by Grants-in-Aid of Scientific Research from the Ministry of Health, Labour, and Welfare of Japan, Grants-in-Aid for Scientific Research from the Ministry of Education, Culture, Sports, Science and Technology of Japan, and Grants-in-Aid of the Japan Science and Technology Agency.

Supplementary data

Supplementary data (^{1}H NMR spectra of final new compounds for **4** and **8**) associated with this article can be found, in the online version, at http://dx.doi.org/10.1016/j.bmc.2014.02.032. These data include MOL files and InChiKeys of the most important compounds described in this article.

References and notes

1. Smalley, W. E.; Ray, W. A.; Daugherty, J. R.; Griffin, M. R. *Am. J. Epidemiol.* **1995**, *141*, 539.
2. Singh, G. *Am. J. Med.* **1998**, *105*, 31S.
3. Kujubu, D. A.; Fletcher, B. S.; Varnum, B. C.; Lim, R. W.; Herschman, H. R. *J. Biol. Chem.* **1991**, *266*, 12866.
4. Xie, W. L.; Chipman, J. G.; Robertson, D. L.; Erikson, R. L.; Simmons, D. L. *Proc. Natl. Acad. Sci. U.S.A.* **1991**, *88*, 2692.
5. Silverstein, F. E.; Faich, G.; Goldstein, J. L.; Simon, L. S.; Pincus, T.; Whelton, A.; Makuch, R.; Eisen, G.; Agrawal, N. M.; Stenson, W. F.; Burr, A. M.; Zhao, W. W.; Kent, J. D.; Lefkowith, J. B.; Verburg, K. M.; Geis, G. S. *JAMA* **2000**, *284*, 1247.
6. Bombardier, C.; Laine, L.; Reicin, A.; Shapiro, D.; Burgos, V. R.; Davis, B.; Day, R.; Ferraz, M. B.; Hawkey, C. J.; Hochberg, M. C.; Kvien, T. K.; Schnitzer, T. J. *N. Engl. J. Med.* **2000**, *343*, 1520.
7. FitzGerald, G. A.; Patrono, C. *N. Engl. J. Med.* **2001**, *345*, 433.
8. Mukherjee, D.; Nissen, S. E.; Topol, E. J. *JAMA* **2001**, *286*, 954.
9. Mukherjee, D. *Biochem. Pharmacol.* **2002**, *63*, 817.
10. McAdam, B. F.; Catella, L. F.; Mardini, I. A.; Kapoor, S.; Lawson, J. A.; FitzGerald, G. A. *Proc. Natl. Acad. Sci. U.S.A.* **1999**, *96*, 272.
11. Catella, L. F.; McAdam, B.; Morrison, B. W.; Kapoor, S.; Kujubu, D.; Antes, L.; Lasseter, K. C.; Quan, H.; Gertz, B. J.; FitzGerald, G. A. *J. Pharmacol. Exp. Ther.* **1999**, *289*, 735.
12. Belton, O.; Byrne, D.; Kearney, D.; Leahy, A.; Fitzgerald, D. J. *Circulation* **2000**, *102*, 840.
13. Garcia Rodriguez, L. A.; Gonzalez-Perez, A. *BMC Med.* **2005**, *3*, 17.
14. Kearney, P. M.; Baigent, C.; Godwin, J.; Halls, H.; Emberson, J. R.; Patrono, C. *BMJ* **2006**, *332*, 1302.
15. Oitate, M.; Hirota, T.; Koyama, K.; Inoue, S.; Kawai, K.; Ikeda, T. *Drug Metab. Dispos.* **2006**, *34*, 1417.
16. Oitate, M.; Hirota, T.; Murai, T.; Miura, S.; Ikeda, T. *Drug Metab. Dispos.* **2007**, *35*, 1846.
17. Oitate, M.; Hirota, T.; Takahashi, M.; Murai, T.; Miura, S.; Senoo, A.; Hosokawa, T.; Oonishi, T.; Ikeda, T. *J. Pharmacol. Exp. Ther.* **2007**, *320*, 1195.
18. Ligumsky, M.; Golanska, E. M.; Hansen, D. G.; Kauffman, G. J. *Gastroenterology* **1983**, *84*, 756.
19. Ligumsky, M.; Sestieri, M.; Karmeli, F.; Zimmerman, J.; Okon, E.; Rachmilewitz, D. *Gastroenterology* **1990**, 1245.
20. Lichtenberger, L. M. *Biochem. Pharmacol.* **2001**, *61*, 631.
21. Tomisato, W.; Tsutsumi, S.; Hoshino, T.; Hwang, H. J.; Mio, M.; Tsuchiya, T.; Mizushima, T. *Biochem. Pharmacol.* **2004**, *67*, 575.
22. Aburaya, M.; Tanaka, K.; Hoshino, T.; Tsutsumi, S.; Suzuki, K.; Makise, M.; Akagi, R.; Mizushima, T. *J. Biol. Chem.* **2006**, *281*, 33422.
23. Tanaka, K.; Tomisato, W.; Hoshino, T.; Ishihara, T.; Namba, T.; Aburaya, M.; Katsu, T.; Suzuki, K.; Tsutsumi, S.; Mizushima, T. *J. Biol. Chem.* **2005**, *280*, 31059.
24. Tsutsumi, S.; Gotoh, T.; Tomisato, W.; Mima, S.; Hoshino, T.; Hwang, H. J.; Takenaka, H.; Tsuchiya, T.; Mori, M.; Mizushima, T. *Cell Death Differ.* **2004**, *11*, 1009.
25. Tomisato, W.; Tanaka, K.; Katsu, T.; Kakuta, H.; Sasaki, K.; Tsutsumi, S.; Hoshino, T.; Aburaya, M.; Li, D.; Tsuchiya, T.; Suzuki, K.; Yokomizo, K.; Mizushima, T. *Biochem. Biophys. Res. Commun.* **2004**, *323*, 1032.
26. Tomisato, W.; Tsutsumi, S.; Rokutan, K.; Tsuchiya, T.; Mizushima, T. *Am. J. Physiol. Gastrointest. Liver Physiol.* **2001**, *281*, G1092.
27. Yamakawa, N.; Suemasu, S.; Matoyama, M.; Kimoto, A.; Takeda, M.; Tanaka, K.; Ishihara, T.; Katsu, T.; Okamoto, Y.; Otsuka, M.; Mizushima, T. *J. Med. Chem.* **2010**, *53*, 7879.
28. Yamakawa, N.; Suemasu, S.; Matoyama, M.; Tanaka, K.-I.; Katsu, T.; Miyata, K.; Okamoto, Y.; Otsuka, M.; Mizushima, T. *Bioorg. Med. Chem.* **2011**, *19*, 3299.
29. Yamakawa, N.; Suemasu, S.; Okamoto, Y.; Tanaka, K.; Ishihara, T.; Asano, T.; Miyata, K.; Otsuka, M.; Mizushima, T. *J. Med. Chem.* **2012**, *55*, 5143.
30. Suemasu, S.; Yamakawa, N.; Ishihara, T.; Asano, T.; Tahara, K.; Tanaka, K.; Matsui, H.; Okamoto, Y.; Otsuka, M.; Takeuchi, K.; Suzuki, H.; Mizushima, T. *Biochem. Pharmacol.* **2012**, *84*, 1470.
31. Yamakawa, N.; Suemasu, S.; Watanabe, H.; Tahara, K.; Tanaka, K.; Okamoto, Y.; Ohtsuka, M.; Maruyama, T.; Mizushima, T. *Drug Metab. Pharmacokinet.* **2013**, *28*, 118.
32. Praveen Rao, P. N.; Amini, M.; Li, H.; Habeeb, A. G.; Knaus, E. E. *J. Med. Chem.* **2003**, *46*, 4872.
33. Abdellatif, K. R.; Chowdhury, M. A.; Dong, Y.; Velazquez, C.; Das, D.; Suresh, M. R.; Knaus, E. E. *Bioorg. Med. Chem.* **2008**, *16*, 9694.
34. Ahlström, M. M.; Ridderström, M.; Zamora, I.; Luthman, K. *J. Med. Chem.* **2007**, *50*, 4444.
35. Penning, T. D.; Talley, J. J.; Bertenshaw, S. R.; Carter, J. S.; Collins, P. W.; Docter, S.; Graneto, M. J.; Lee, L. F.; Malecha, J. W.; Miyashiro, J. M.; Rogers, R. S.; Rogier, D. J.; Yu, S. S.; Anderson, G. d.; Burton, E. G.; Cogburn, J. N.; Gregory, S. A.; Koboldt, C. M.; Perkins, W. E.; Seibert, K.; Veenhuizen, A. W.; Zhang, Y. Y.; Isakson, P. C. *J. Med. Chem.* **1997**, *40*, 1347.
36. Gosselin, F.; O'Shea, P. D.; Webster, R. A.; Reamer, R. A.; Tillyer, R. D.; Grabowski, E. J. J. *Synlett* **2006**, 3267.
37. Uddin, M. J.; Rao, P. N. P.; Knaus, E. E. *J. Heterocycl. Chem.* **2003**, *40*, 861.
38. Zarghi, A.; Rao, P. N.; Knaus, E. E. *J. Pharm. Pharm. Sci.* **2007**, *10*, 159.
39. Abdellatif, K. R.; Huang, Z.; Chowdhury, M. A.; Kaufman, S.; Knaus, E. E. *Bioorg. Med. Chem. Lett.* **2011**, *21*, 3951.

SCIENTIFIC REPORTS

OPEN

SUBJECT AREAS:
DRUG DEVELOPMENT
TRANSLATIONAL RESEARCH
EXPERIMENTAL MODELS OF DISEASE

Received
20 November 2013

Accepted
12 March 2014

Published
28 March 2014

Correspondence and requests for materials should be addressed to T.M. (mizushima-th@pha.keio.ac.jp)

Superiority of pulmonary administration of mepenzolate bromide over other routes as treatment for chronic obstructive pulmonary disease

Ken-Ichiro Tanaka[1], Shota Kurotsu[1], Teita Asano[1], Naoki Yamakawa[1], Daisuke Kobayashi[1], Yasunobu Yamashita[1], Hiroshi Yamazaki[1], Tomoaki Ishihara[1], Hiroshi Watanabe[2], Toru Maruyama[2], Hidekazu Suzuki[3] & Tohru Mizushima[1]

[1]Faculty of Pharmacy, Keio University, Tokyo 105-8512, Japan, [2]Faculty of Life Sciences, Kumamoto University, Kumamoto 862-0973, Japan, [3]Department of Internal Medicine, Keio University School of Medicine, Tokyo 160-8582, Japan.

We recently proposed that mepenzolate bromide (mepenzolate) would be therapeutically effective against chronic obstructive pulmonary disease (COPD) due to its both anti-inflammatory and bronchodilatory activities. In this study, we examined the benefits and adverse effects associated with different routes of mepenzolate administration in mice. Oral administration of mepenzolate caused not only bronchodilation but also decreased the severity of elastase-induced pulmonary emphysema; however, compared with the intratracheal route of administration, about 5000 times higher dose was required to achieve this effect. Intravenously or intrarectally administered mepenzolate also showed these pharmacological effects. The intratracheal route of mepenzolate administration, but not other routes, resulted in protective effects against elastase-induced pulmonary damage and bronchodilation at a much lower dose than that which affected defecation and heart rate. These results suggest that the pulmonary route of mepenzolate administration may be superior to other routes (oral, intravenous or intrarectal) to treat COPD patients.

Chronic obstructive pulmonary disease (COPD) is a serious health problem and the most important etiologic factor of which is cigarette smoke (CS). COPD is currently the fourth leading cause of death in the world and its prevalence and mortality rates are steadily increasing[1]. This disease state is defined by a progressive and not fully reversible airflow limitation associated with an abnormal inflammatory response-mediated permanent enlargement of the pulmonary airspace[1–3]. Thus, for the clinical treatment of COPD, it is important not only to improve the airflow limitation by bronchodilation, but also to suppress disease progression by controlling inflammatory processes.

Bronchodilators (β_2-agonists and muscarinic antagonists) are currently used for the treatment of COPD owing to their ameliorating effects on airflow limitation[2,4,5]. Steroids are also used to suppress inflammatory processes in COPD patients; however steroids do not significantly modulate disease progression or mortality[5,6], because the inflammation associated with COPD tends to be resistant to steroid treatment[7]. Thus, the development of new types of anti-inflammatory drugs to treat COPD is paramount.

The number of drugs reaching the marketplace each year is decreasing, mainly due to the unexpected adverse effects of potential drugs being revealed at advanced clinical trial stages. For this reason, we proposed a new strategy for drug discovery and development (drug re-positioning)[8]. In this strategy, compounds with therapeutically beneficial activity are screened from a library of approved medicines to be developed for new indications. The advantage of this approach is that there is a decreased risk for unexpected adverse effects in humans because the safety aspects of these drugs have already been well characterized in humans[8]. From a library of approved medicines, we screened compounds that prevent elastase-induced pulmonary emphysema in mice, and selected mepenzolate bromide (mepenzolate)[9], which is an orally administered muscarinic receptor antagonist used to treat gastrointestinal disorders (such as peptic ulcers and irritable bowel syndrome)[10–12]. We showed that mepenzolate not only exerts an anti-inflammatory effect via a muscarinic receptor-independent mechanism, but also a bronchodilatory effect via a muscarinic receptor-dependent mechanism[9].

Oxidative stress, such as superoxide anion, is believed to play a major role in abnormal inflammation in COPD patients and nicotinamide adenine dinucleotide phosphate (NADPH) oxidase plays an important role in the production of superoxide anions[13]. The body contains a number of endogenous anti-oxidant proteins such as superoxide dismutase and glutathione S-transferase, with a decrease in these proteins reported to be involved in the pathogenesis of COPD[14,15]. We reported that mepenzolate not only suppressed the elastase-induced production of superoxide anions and NADPH oxidase activation but also stimulated the expression of superoxide dismutase and glutathione S-transferase, suggesting that mepenzolate suppresses elastase-induced pulmonary emphysema via decrease of oxidative stress[9]. Based on these results, we proposed that mepenzolate could serve as a candidate drug for the treatment of COPD.

The route of administration of each particular drug is an important factor to be taken into account when considering its final clinical application. Most muscarinic receptor antagonists currently used for treating COPD patients are administered via the lung[16] because the systemic administration of this type of drug frequently results in adverse effects on cardiac and intestinal functions (such as arrhythmia, heart palpitations and constipation). In this way, we chose the pulmonary route of mepenzolate administration (intratracheal administration or inhalation) in our previous study on mice[9]. On the other hand, since mepenzolate was approved for use as an orally administered drug, the development of this drug to be taken orally for COPD would be more convenient compared to other administration routes. Thus, to determine the appropriate route of mepenzolate administration for possible use by COPD patients, we examined here the effect of different administration routes on this drug's beneficial and adverse effects in mice. When administered intratracheally, mepenzolate showed protective effects on elastase-induced pulmonary damage at a much lower dose than that which affected fecal pellet output and heart rate. With respect to the other administration routes (oral, intravenous and intrarectal), mepenzolate showed protective and adverse effects at similar doses. These results suggest that the pulmonary administration route for mepenzolate may be superior to other routes to treat COPD patients.

Results

Effect of different administration routes of mepenzolate on pulmonary damage and airway resistance. We recently reported that the intratracheal administration or inhalation of mepenzolate suppressed porcine pancreatic elastase (PPE)-induced inflammatory responses, pulmonary emphysema, alteration of lung mechanics, and respiratory dysfunction[9]. As a first step in the present study, we confirmed these effects of intratracheally administered mepenzolate.

As shown in Fig. 1a, the total number of leucocytes and the individual number of neutrophils in bronchoalveolar lavage fluid (BALF), which serve as indicators of pulmonary inflammatory responses, increased after the PPE treatment; this increase was partially suppressed by the simultaneous intratracheal administration of mepenzolate (38 or 190 μg/kg). Histopathological analysis revealed that while PPE administration damaged the alveolar walls and increased mean linear intercept (MLI), this effect could again be partly suppressed by the administration of mepenzolate (38–940 μg/kg; Fig. 1b and c). The alteration of lung mechanics associated with pulmonary emphysema is characterized by a decrease in elastance[17]. PPE treatment decreased both total respiratory system elastance (whole lung elastance, including the bronchi, bronchioles and alveoli) and tissue elastance (elastance of alveoli), both of which were partially restored by simultaneous mepenzolate administration (Fig. 1d). PPE treatment also decreased the $FEV_{0.05}$/FVC ratio (Fig. 1d), which is homologous to the FEV_1/FVC ratio in humans[18,19]. Mepenzolate administration restored the $FEV_{0.05}$/FVC ratio towards control values (Fig. 1d). The bronchodilation activity exerted by mepenzolate was monitored by its inhibitory effect on the increase in airway resistance induced by methacholine[9]. As shown in Fig. 1e, the methacholine-induced increase in airway resistance was completely suppressed by the intratracheal administration of mepenzolate, with the dose required to decrease the airway resistance (0.3 μg/kg) being much lower than that required to protect the pulmonary tissue against PPE-induced damage (38 μg/kg, Fig. 1c). The results in Fig. 1 are thus consistent with those reported previously[9].

We subsequently examined the effects of orally administered mepenzolate on the same parameters as those described above. As shown in Fig. 2a–c, orally administered mepenzolate protected against PPE-induced inflammatory responses and pulmonary emphysema; however, the dose required to achieve this protective effect (190 mg/kg) was much higher than that found when the drug was administered intratracheally (Fig. 1a–c). Orally administered mepenzolate also suppressed PPE-induced alterations of lung mechanics but did not significantly affect respiratory dysfunction (Fig. 2d). The bronchodilatory effect of orally administered mepenzolate was also observed only at higher doses (Fig. 2e) compared with that obtained with intratracheal mepenzolate administration (Fig. 1e). Furthermore, in contrast to the results for intratracheal administration, orally administered mepenzolate showed both bronchodilatory and protective effects against PPE-induced pulmonary disorders at roughly similar doses (Fig. 2).

We also examined the effects of intravenously administered mepenzolate. As shown in Fig. 3a–c, this route of mepenzolate administration (10 μg/kg) protected against PPE-induced inflammatory responses and pulmonary emphysema. Compared to the intratracheal administration, although the effective dose was slightly lower via the intravenous route, the extent of amelioration was not as apparent (Fig. 3a–c). Furthermore, intravenous administration of the highest dose of mepenzolate tested for this route (100 μg/kg) did not protect against PPE-induced pulmonary damage (Fig. 3a and c), nor did it significantly restore the lung mechanics and respiratory function, both of which were affected by the PPE treatment (Fig. 3d). These results demonstrate that intravenously administered mepenzolate is not as effective against PPE-induced pulmonary damage as that achieved via the intratracheally administered route. On the other hand, almost complete inhibition of the methacholine-induced increase in airway resistance was observed with the intravenous administration of mepenzolate (Fig. 3e). These results suggest that the protective effects of mepenzolate against PPE-induced pulmonary damage and its bronchodilatory effect are independent of each other.

Monitoring of the mepenzolate level in blood and tissue after administration of the drug via different routes. High performance liquid chromatography (HPLC) analysis was used to determine the level of mepenzolate in plasma and tissue. We initially examined the plasma level of mepenzolate after its intravenous administration, with the detected levels of the drug increasing in a dose-dependent manner (Fig. 4a). Examination of the time-course profile showed that mepenzolate was clearly detectable at 1 min, significantly reduced after 5 min, and undetectable 30 min following its intravenous administration (Fig. 4b), suggesting that mepenzolate is very unstable in blood. We then performed similar analyses to determine plasma mepenzolate levels after oral administration of the drug. As shown in Fig. 4c, mepenzolate could be detected in the plasma only when a very high dose (940 mg/kg) of the drug was administered via this route. Furthermore, the peak level was achieved 30 min after oral administration (Fig. 4d). In contrast, when mepenzolate was administered via the intratracheal route, it could be detected at a relatively lower dose (10 mg/kg) (Fig. 4e). Furthermore, the detection was very rapidly (at 1 min) (Fig. 4f). These results suggests that the efficiency of absorption into the circulation is higher for the intratracheal route of administration than the oral route. We also tried to detect mepenzolate in the lung tissue of treated mice, with the drug detected following

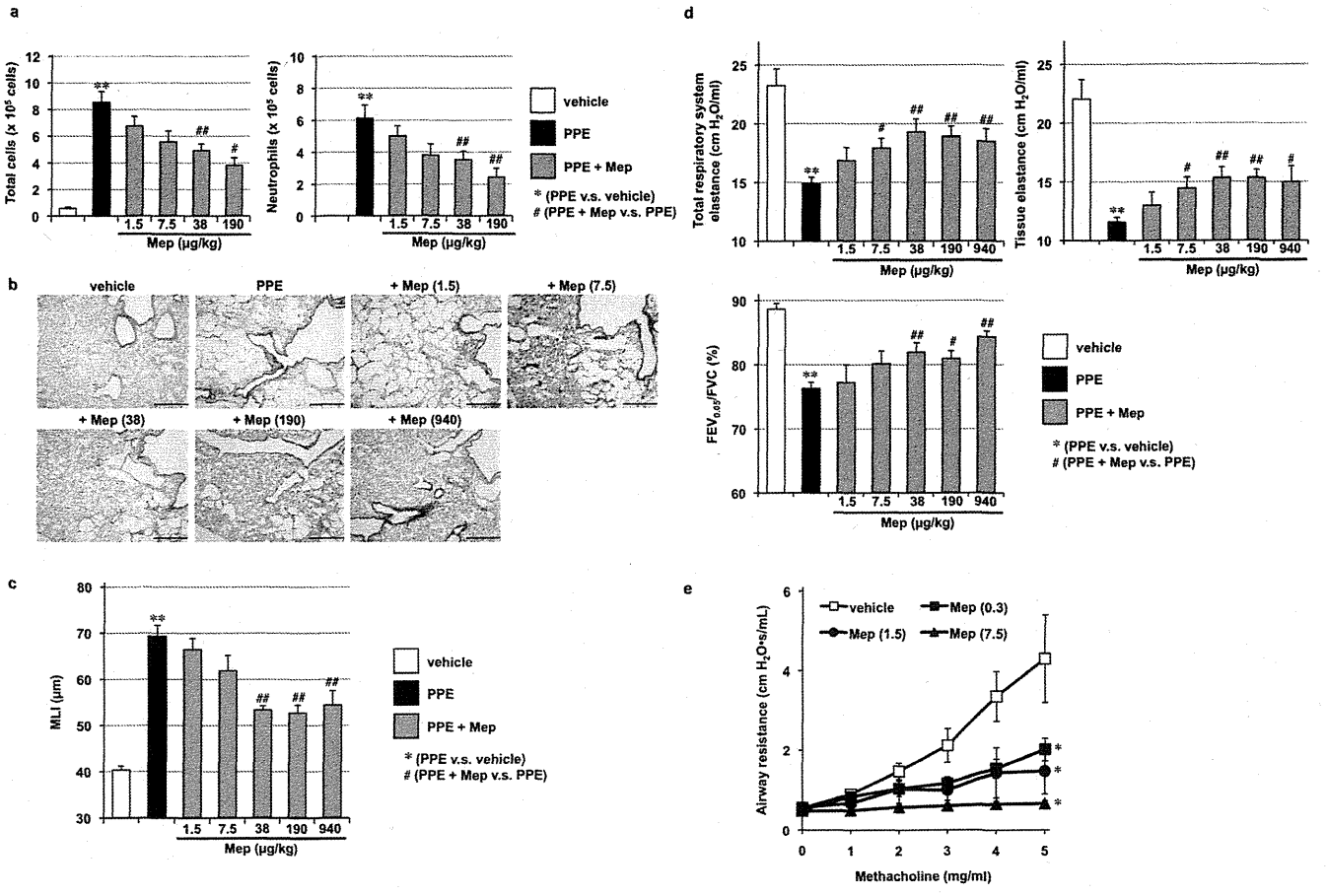

Figure 1 | Effect of intratracheal administration of mepenzolate on PPE-induced pulmonary damage and methacholine-induced airway constriction. Mice were treated with or without (vehicle) PPE (15 U/kg) once only on day 0 (a–d). The indicated doses (μg/kg) of mepenzolate (Mep) were administered intratracheally once only (a) or once daily for 12 days (from day 0 to day 11) (b–d). Twenty-four hours after the PPE administration, BALF was prepared and the total cell number and the number of neutrophils were determined as described in the Materials and Methods (a). Sections of pulmonary tissue were prepared on day 14 and subjected to histopathological examination (H & E staining) (scale bar, 500 μm) (b). Airspace size was estimated by determining the MLI as described in the Materials and Methods (c). Total respiratory system elastance, tissue elastance, and $FEV_{0.05}$/FVC were determined on day 14 as described in the Materials and Methods (d). Indicated doses (μg/kg) of mepenzolate (Mep) were administered intratracheally. After 1 h, mice were exposed to nebulized methacholine 5 times and airway resistance was determined after each methacholine challenge as described in the Materials and Methods (e). Values represent mean 6 S.E.M. (n 5 3–10). * or # P , 0.05; ** or ## P , 0.01.

administration via the intratracheal route (Fig. 4g), but not for orally or intravenously administered drug (data not shown). The results in Fig. 4g also showed that most of intratracheally administered mepenzolate disappeared from the lung within 30 min.

Effect of intrarectally administered mepenzolate on pulmonary damage and airway resistance. It has been reported that, compared to the oral route of administration, the intrarectal route for some drugs results in a much higher uptake efficiency into the circulation due to the circumvention of drug inactivation within the gastrointestinal tract and the first-pass effect, or the higher efficiency of absorption via the rectum compared with the small intestine[20,21]. For these reasons, we examined the effect of intrarectally administered mepenzolate on PPE-induced pulmonary damage and airway resistance. As shown in Fig. 5a–c, intrarectally administered mepenzolate showed a protective effect against PPE-induced pulmonary damage at doses of 1.5 or 7.5 mg/kg, which are much lower than that required in the case of oral administration (Fig. 2a–c). Similar results were observed with respect to the PPE-induced alteration of lung mechanics and respiratory dysfunction; however, the amelioration of respiratory function by intrarectally administered mepenzolate was not statistically significant (Fig. 5d). As shown in Fig. 5e, intrarectally administered mepenzolate suppressed the methacholine-induced increase in airway resistance at lower doses to that seen in response to oral administration of the drug (Fig. 2e).

We also determined the plasma level of mepenzolate after the intrarectal administration of this drug. The dose-response and time-course profiles (Fig. 5f and g) revealed that the absorption into the circulation of intrarectally administered mepenzolate is much more efficient and rapid than that seen with orally administered drug (Fig. 4c and d). The results in Fig. 5 thus suggest that the intrarectal route of mepenzolate administration is more effective than the oral route due to the lower effective doses required.

We also examined the effect of different routes of mepenzolate administration on CS-induced lung inflammatory responses. As shown in Fig. 6a, the total number of leucocytes and the individual number of macrophages in BALF increased after the CS treatment and this increase was suppressed by the simultaneous intratracheal administration of mepenzolate (38 or 190 μg/kg). Similar suppression was observed with oral, intravenous or intrarectal administration of mepenzolate (Fig. 6b–d), however, the oral administration required much higher dose of mepenzolate than the intratracheal administration (Fig. 6a, b). Furthermore, the extent of suppression was not so apparent with the intravenous or intrarectal administration as the intratracheal administration and the suppression of

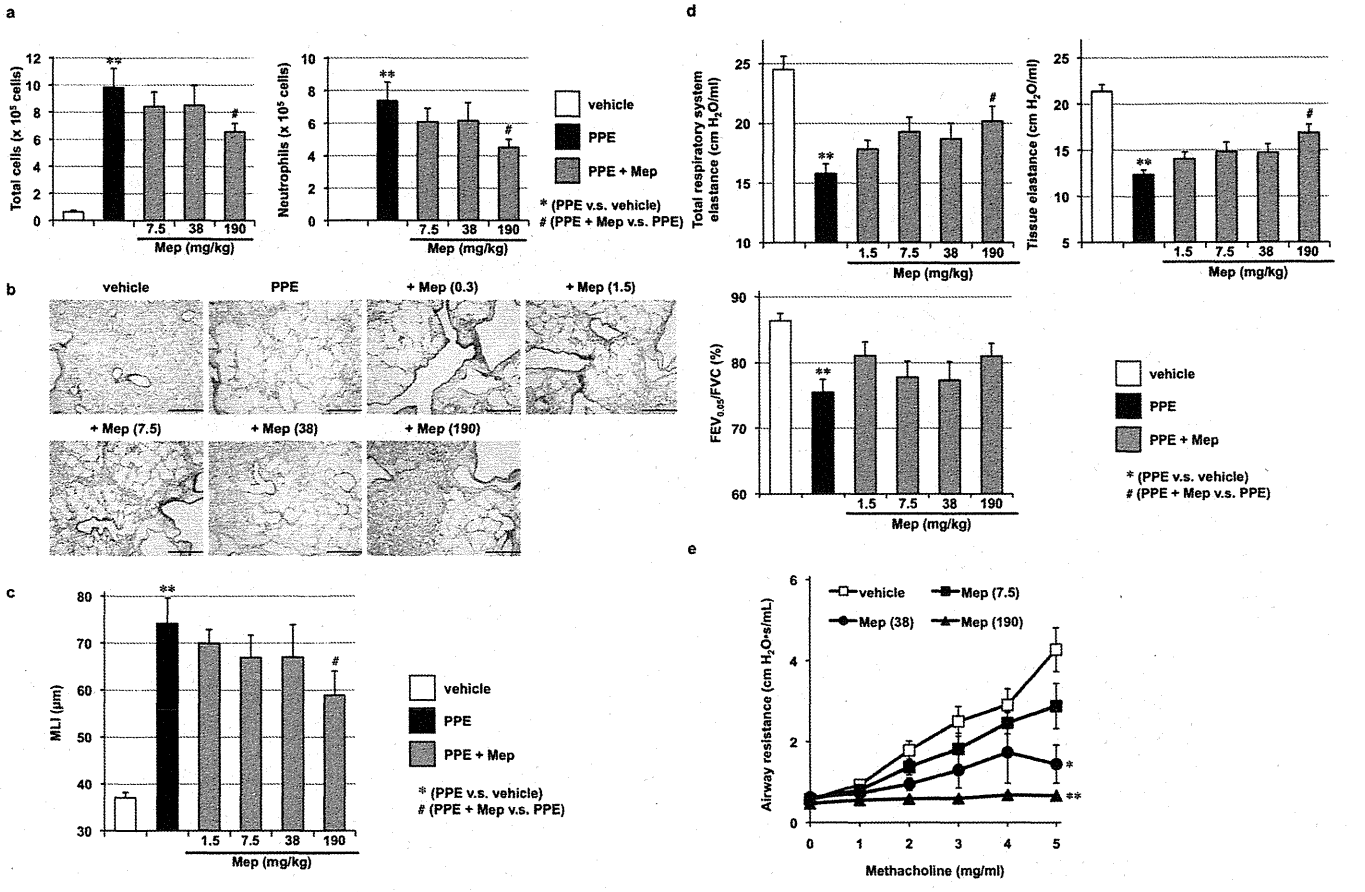

Figure 2 | Effect of oral administration of mepenzolate on PPE-induced pulmonary damage and methacholine-induced airway constriction. Administration of PPE, mepenzolate and methacholine was performed as described in the legend of Fig. 1, except that mepenzolate was administered orally (a⊠). Analysis of inflammatory responses (a), histopathological examination (scale bar, 500 μm) (b), determination of the MLI (c), measurement of lung mechanics and respiratory function (d) and measurement of airway resistance (e) were carried out as described in the legend of Fig. 1. Values represent mean 6 S.E.M. (n 5 3⊠). * or # P , 0.05; ** P , 0.01.

increase in the total number of leucocytes and the individual number of macrophages in BALF by intravenous administration of mepenzolate (10 or 100 μg/kg) was not statistically significant (Fig. 6).

Effect of different administration routes of mepenzolate on the appearance of adverse effects. To determine the appropriate administration route of any drug, it is important to consider not only its beneficial but also its adverse side-effects. For the clinical application of mepenzolate to treat COPD patients, both constipation and arrhythmia (heart palpitations) have been noted as adverse side-effects that occur due to the inhibitory effects of this drug on the muscarinic receptor and the resulting inhibition of intestinal motility and increased heart rate[22,23]. We therefore examined the effect of different routes of mepenzolate administration on defecation and heart rate in treated mice.

Mice were subjected to restraint stress as a means to increase fecal pellet output. As shown in Fig. 7, mepenzolate administration suppressed fecal pellet output with respect to control (untreated) mice for each of the routes tested. Compared to the protective effects exerted by mepenzolate against PPE-induced pulmonary damage (Fig. 1), doses administered via the intratracheal administration route that were more than 100 times higher were required to affect fecal pellet output (Fig. 7a). In contrast, less than one hundredth the dose of mepenzolate required to provide a protective effect against lung damage significantly affected fecal pellet output when the oral administration route was used (Fig. 7b). As for the intravenous or intrarectal routes of administration, roughly similar doses of mepenzolate were required for both inhibition of fecal pellet output and protection against PPE-induced pulmonary damage (Figs. 3c, 5c, 7c and 7d). These results suggest that intratracheally administered mepenzolate could protect against PPE-induced pulmonary damage without affecting gut motility. Moreover, the results also suggest that orally administered mepenzolate affects gut motility directly (but not after absorption), because the dose required to suppress fecal pellet output was much lower compared to that required for other pharmacological effects.

Lastly, we examined the effect of mepenzolate on heart rate as measured by infrared sensor. As shown in Fig. 8a, intratracheally administered mepenzolate increased heart rate only at a dose that was much higher than that required to protect against PPE-induced pulmonary damage (Fig. 1c). On the other hand, the oral, intravenous or intrarectal routes of mepenzolate administration increased the heart rate at doses roughly similar to that required for pulmonary protection (Figs. 2c, 3c, 5c, 8b–d). These results suggest that intratracheally administered mepenzolate protects against PPE-induced pulmonary damage without affecting heart rate.

Discussion

Since COPD is characterized by airflow limitation and abnormal inflammatory responses, a combination of anti-inflammatory drugs (such as steroids) and bronchodilators is the standard treatment regime[24,25]. Since mepenzolate has both anti-inflammatory and bronchodilatory activities, this drug may be beneficial for treating COPD without the concomitant use of other drugs. In particular, the anti-inflammatory effect of mepenzolate is an important property of this drug, because the inflammation associated with COPD tends to

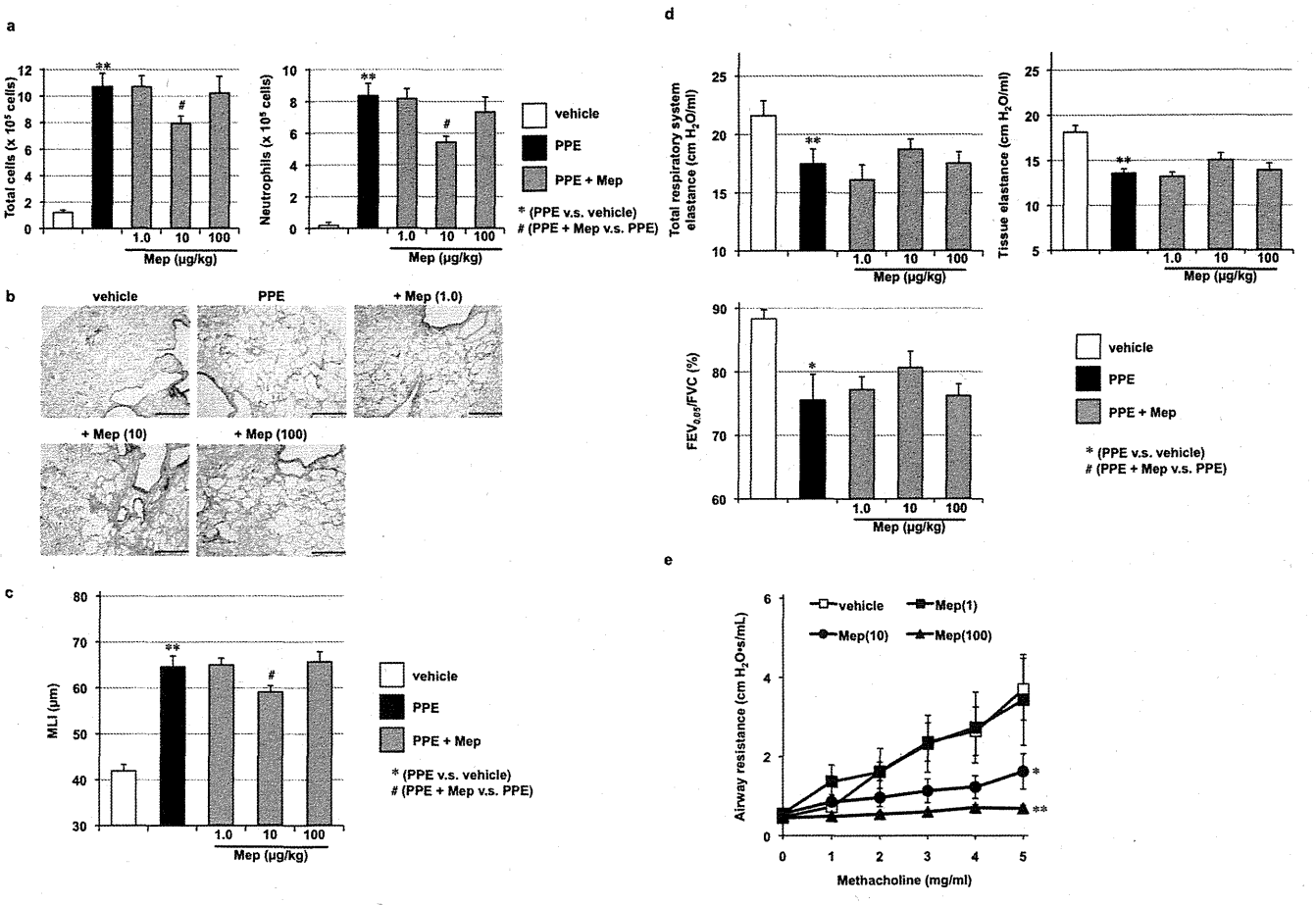

Figure 3 | Effect of intravenous administration of mepenzolate on PPE-induced pulmonary damage and methacholine-induced airway constriction. Administration of PPE, mepenzolate and methacholine was performed as described in the legend of Fig. 1, except that mepenzolate was administered intravenously (a□4). Analysis of inflammatory responses (a), histopathological examination (scale bar, 500 μm) (b), determination of the MLI (c), measurement of lung mechanics and respiratory function (d) and measurement of airway resistance (e) were carried out as described in the legend of Fig. 1. Values represent mean 6 S.E.M. (n 5 3□4). * or # P , 0.05; ** P , 0.01.

show resistance to steroid treatment; common steroids as such do not significantly modulate disease progression and mortality[5–7]. This insensitivity to steroids can be explained by the notion that steroids suppress the expression of pro-inflammatory genes via their action on histone deacetylase (HDAC) 2[26,27]. CS also inhibits the activity and expression of HDAC2[26]. On the other hand, mepenzolate can restore HDAC activity under inflammatory conditions[9], which may explain its superior anti-inflammatory activity to steroids under these conditions (see below). In an animal model of elastase-induced lung inflammation and emphysema, we reported that steroids do not provide protective or therapeutic benefits against PPE-induced pulmonary emphysema, alterations of lung mechanics, or respiratory dysfunction[19], whereas mepenzolate was effective against these disorders under the same experimental conditions[9]. Based on these results, we considered that mepenzolate could be therapeutically beneficial to treat COPD patients, which motivated us to examine here the effect of different routes of mepenzolate administration (intratracheal, oral, intravenous or intrarectal) on its beneficial effects (protection against PPE-induced pulmonary damage and bronchodilation) and adverse side-effects (alteration of gut motility and heart rate) in mice.

Intratracheally administered mepenzolate protected against PPE-induced pulmonary damage (inflammatory responses, pulmonary emphysema, alteration of lung mechanics and respiratory dysfunction) at a dose of 38 μg/kg and showed bronchodilation activity at a dose of 0.3 μg/kg, as reported recently[9]. We here found that this mode of administration required a much higher dose (4.7 mg/kg) to affect fecal pellet output and heart rate, thus demonstrating that intratracheally administered mepenzolate could suppress PPE-induced pulmonary damage and improve airflow limitation without affecting these other parameters, which is of particular clinical significance in terms of the use of this drug to treat COPD patients. This may be due to the fact that intratracheally administered mepenzolate is localized within the lung, in contrast to the other routes of administration studied. Furthermore, the lower dose of mepenzolate required for bronchodilation (compared to protection against PPE-induced pulmonary damage) suggests that intratracheally administered mepenzolate is localized within the bronchi rather than the alveoli, because such differences in dosage were not observed for the other forms of systemic administration.

We found here that the oral and intravenous routes of mepenzolate administration also protected against PPE-induced pulmonary damage and showed bronchodilatory activity. However, the improvement of respiratory function ($FEV_{0.05}$/FVC) by mepenzolate was not statistically significant when the drug was administered via these routes. Compared to intravenous or intratracheal administration, much higher doses of mepenzolate were required to protect against PPE-induced pulmonary damage for the oral route of administration, suggesting that the efficiency of absorption into the circulation is very poor for administration via this route. It should be noted that mepenzolate achieved beneficial and adverse effects at roughly similar doses when administered orally or intravenously (except for the effect of orally administered mepenzolate on fecal pellet output). When the route of administration was intrarectal rather than oral,

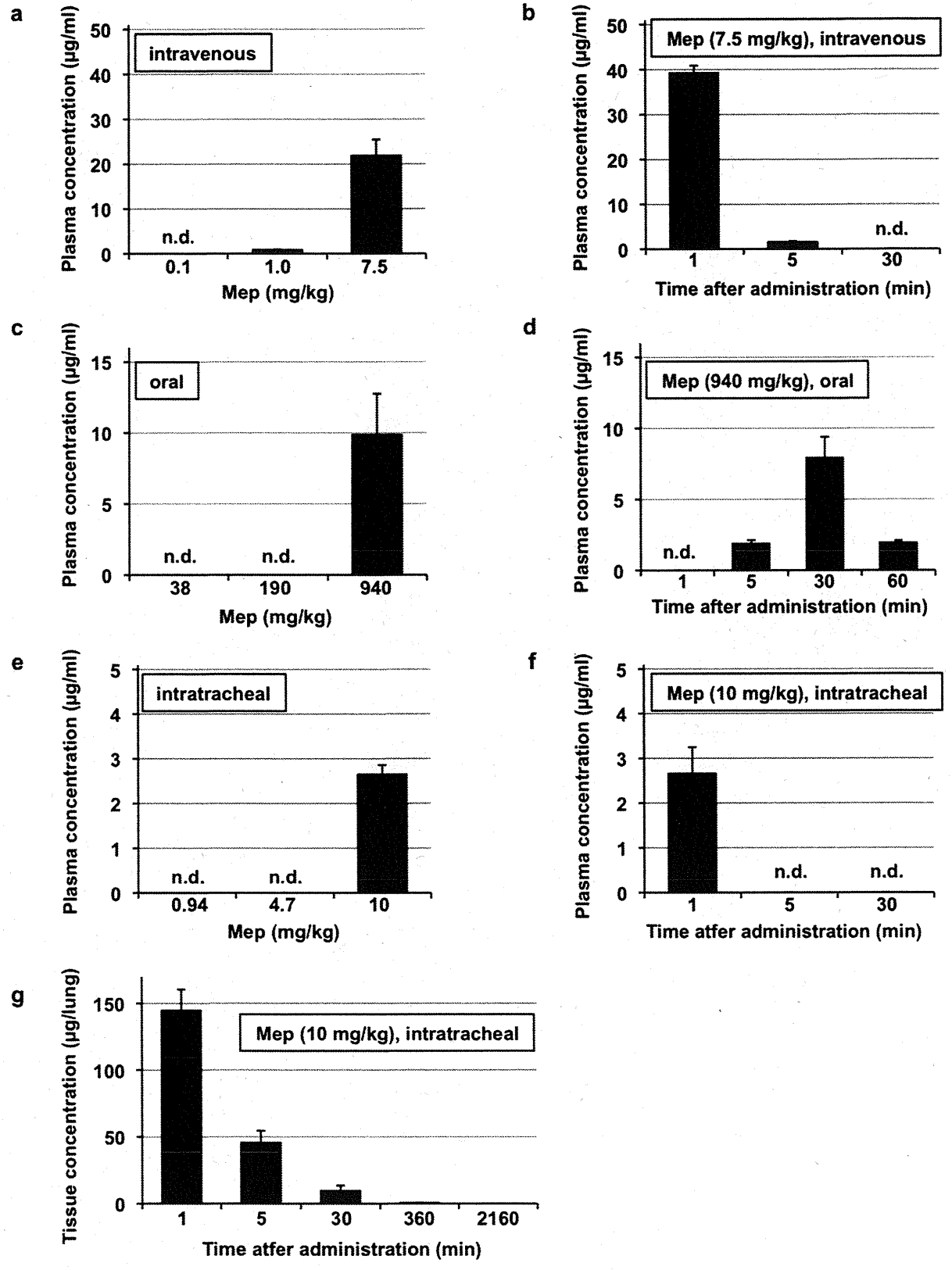

Figure 4 | Determination of the level of mepenzolate after administration through various routes. Mice were administered indicated doses of mepenzolate intravenously (a, b), orally (c, d) or intratracheally (e–g). After indicated periods (b, d, f, g), 1 min (a, e) or 30 min (c), blood samples (a–f) or lung homogenates (g) were prepared and the level of mepenzolate was determined as described in the Materials and Methods. Values are mean 6 S.E.M. (n 5 3–4). n.d., not detected.

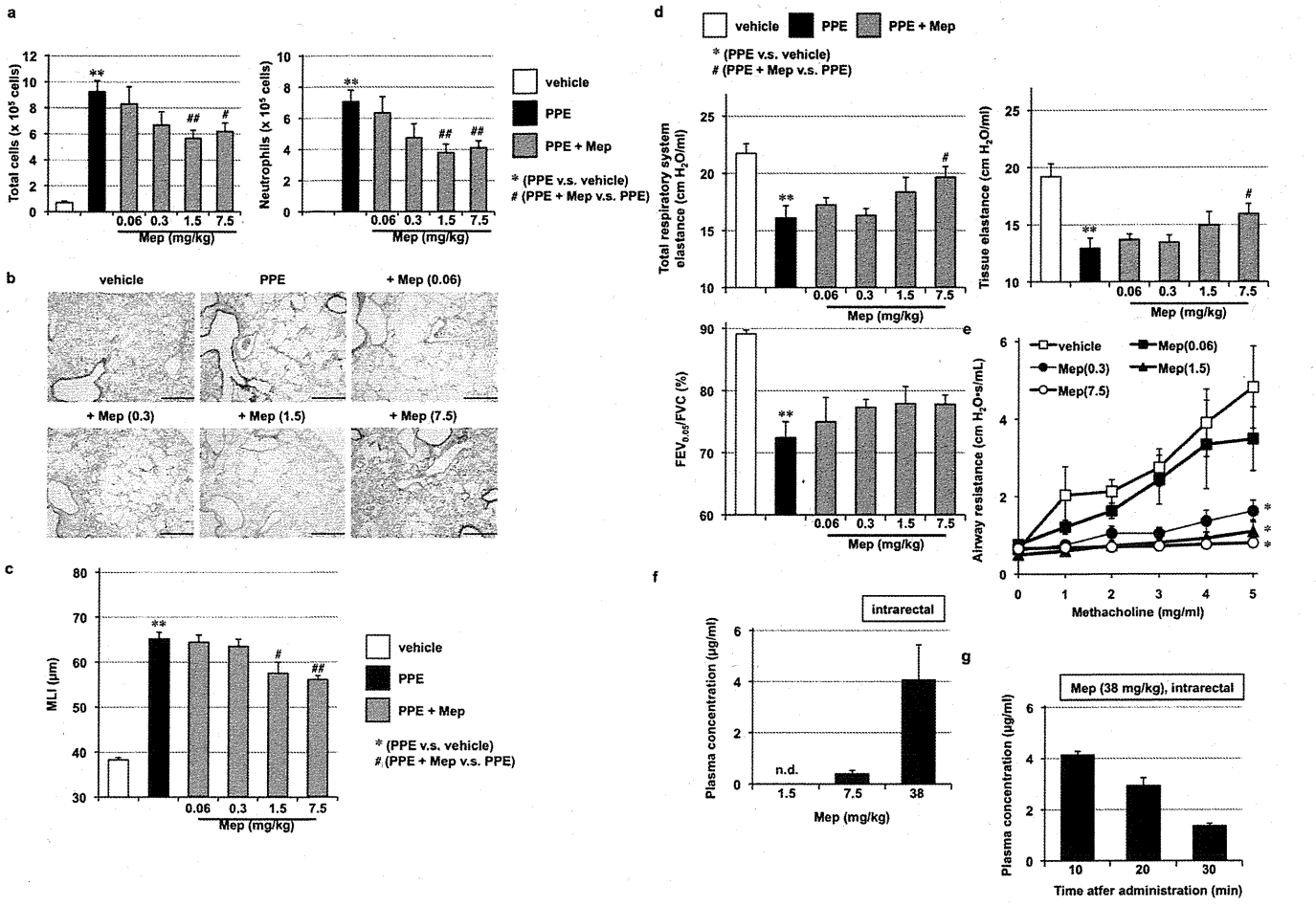

Figure 5 | Effect of intrarectal administration of mepenzolate on PPE-induced pulmonary damage and methacholine-induced airway constriction. Administration of PPE, mepenzolate and methacholine was done, as described in the legend of Fig. 1, except that mepenzolate was administered intrarectally (a⊠e). Analysis of inflammatory responses (a), histopathological examination (scale bar, 500 μm) (b), determination of the MLI (c), measurement of lung mechanics and respiratory function (d) and measurement of airway resistance (e) were carried out as described in the legend of Fig. 1. Mice were administered indicated doses of mepenzolate intrarectally. After 10 min (f) or indicated periods (g), blood samples were taken and the plasma level of mepenzolate was monitored as described in the legend of Fig. 4. Values represent mean 6 S.E.M. (n 5 4⊠12). * or $^{\#}$P , 0.05; ** or $^{\#\#}$P , 0.01; n.d., not detected.

the effective dose of mepenzolate was decreased. However, as for the oral and intravenous routes of administration, intrarectally administered mepenzolate exerted both beneficial and adverse side-effects at roughly similar doses.

To determine the appropriate administration route of candidate drugs in a clinical setting, the most important factor is the balance between efficacy and safety. To estimate this factor in animals, the ratio between doses showing adverse effects and efficacy is useful. We calculated this index (Table 1) and results show the superiority of the pulmonary administration route for mepenzolate compared to other routes. The quality of life (QOL) of patients is also an important factor, for which the intravenous route of administration has a disadvantage. As well as oral administration, pulmonary administration (such as inhalation) would not overly affect the QOL of COPD patients given that most of these patients would already be required to take bronchodilators and/or steroids on a daily basis at home through inhalation.

On the other hand, one of the main advantages of the oral route of mepenzolate administration is that it already has regulatory approval, and most pre-clinical tests (such as toxicity and pharmacokinetic tests) could be omitted if the dose for a new indication (COPD) is less than that for the approved indication (gastrointestinal disorders). However, we found that the dose of orally administered drug required to protect against PPE-induced pulmonary damage was much higher than that at which fecal pellet output is affected, suggesting that the clinical dose of mepenzolate for the treatment of COPD would be higher than the already approved dosage. On the other hand, if mepenzolate is developed as a drug to be administered via the pulmonary route, although some pre-clinical tests (such as toxicity and pharmacokinetic tests) are required, other tests (such as genotoxicity tests) could be omitted. Furthermore, because the dose required to protect against PPE-induced pulmonary damage via the intratracheal route was much lower than the orally administered dose that affects fecal pellet output, it could be postulated that the clinical dose of mepenzolate required for the treatment of COPD patients may be lower than the already approved dose if this drug is developed as a drug to be administered intrapulmonary. This could decrease the risk of adverse effects in a clinical setting. In conclusion, we propose that the pulmonary administration of mepenzolate may be superior to other administration routes for the treatment of COPD.

Methods

Chemicals and animals. Mepenzolate, PPE and HPLC-grade acetonitrile were obtained from Sigma-Aldrich (St. Louis, MO). Novo-Heparin for injection was from Mochida Pharmaceutical Co. (Tokyo, Japan). Chloral hydrate was from Nacalai Tesque (Kyoto, Japan). Diff-Quik was from the Sysmex Co (Kobe, Japan). Sodium 1-propanesulfonate was from Tokyo Kasei Chemical Co (Tokyo, Japan). The Amicon utra-0.5 centrifugal filter unit was purchased from Merck Millipore (Billerica, MA).

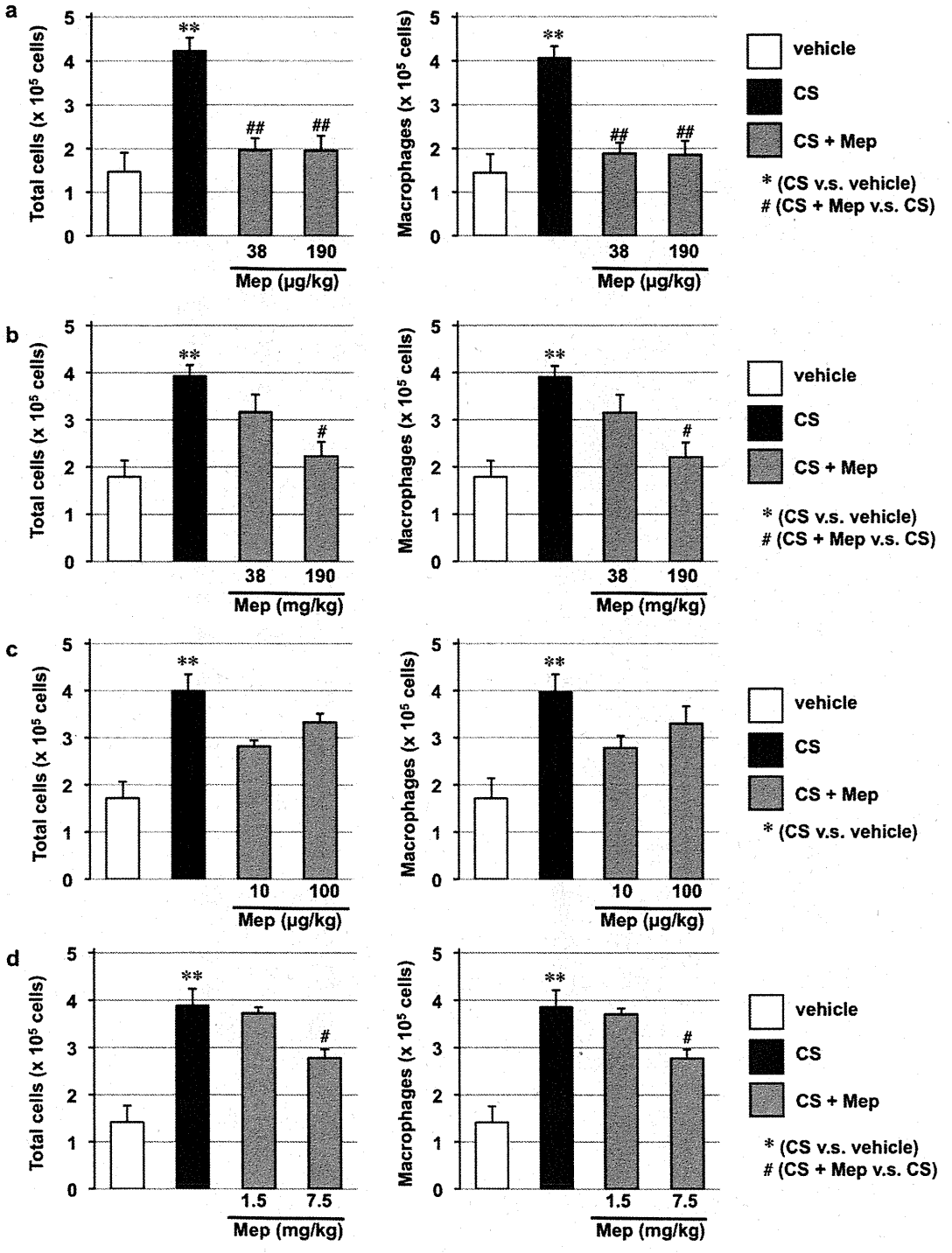

Figure 6 | Effect of mepenzolate on CS-induced pulmonary inflammatory responses. Mice were exposed to CS (3 times/day) and intratracheally (a), orally (b), intravenously (c) or intrarectally (d) administered indicated dose of mepenzolate (once daily) for 3 days as described in the Materials and Methods. Six hours after the last CS exposure, BALF was prepared and the total cell number and the number of macrophages were determined as described in the Materials and Methods. Values represent mean 6 S.E.M. (n5 4⊠). * or #P, 0.05; ** or ##P, 0.01.

Formalin neutral buffer solution, potassium dihydrogen phosphate and methylcellulose were from WAKO Pure Chemicals (Tokyo, Japan). Mayer's hematoxylin, 1% eosin alcohol solution and malinol were from MUTO Pure Chemicals (Tokyo, Japan). ICR mice (4–6 weeks old, male) were purchased from Charles River (Yokohama, Japan). The experiments and procedures described here were carried out in accordance with the Guide for the Care and Use of Laboratory Animals as adopted and promulgated by the National Institutes of Health, and were approved by the Animal Care Committee of Keio University.

Treatment of mice with PPE, CS and drugs. Mice maintained under anesthesia with chloral hydrate (500 mg/kg) were given one intratracheal administration of PPE (15 U/kg) and mepenzolate (various doses) in PBS (1 ml/kg) via micropipette. For control mice, PBS alone was administered by the same procedure.

ICR mice were exposed to CS by placing 15–20 mice in a chamber (volume, 45 L) connected to a CS-producing apparatus. Commercial non-filtered cigarettes (Peace; Japan Tobacco Inc., Tokyo, Japan) that yielded 28 mg tar and 2.3 mg nicotine on a standard smoking regimen were used. Mice were exposed to the smoke of 2 cigarettes for 20 min, 3 times/day for 3 days. The apparatus was configured such that each cigarette was puffed 15 times over a 5 min period.

For the oral or intrarectal mode of administration, mepenzolate (various doses) in 1% methylcellulose was administered by sonde. For control mice, 1% methylcellulose alone was administered by the same procedure.

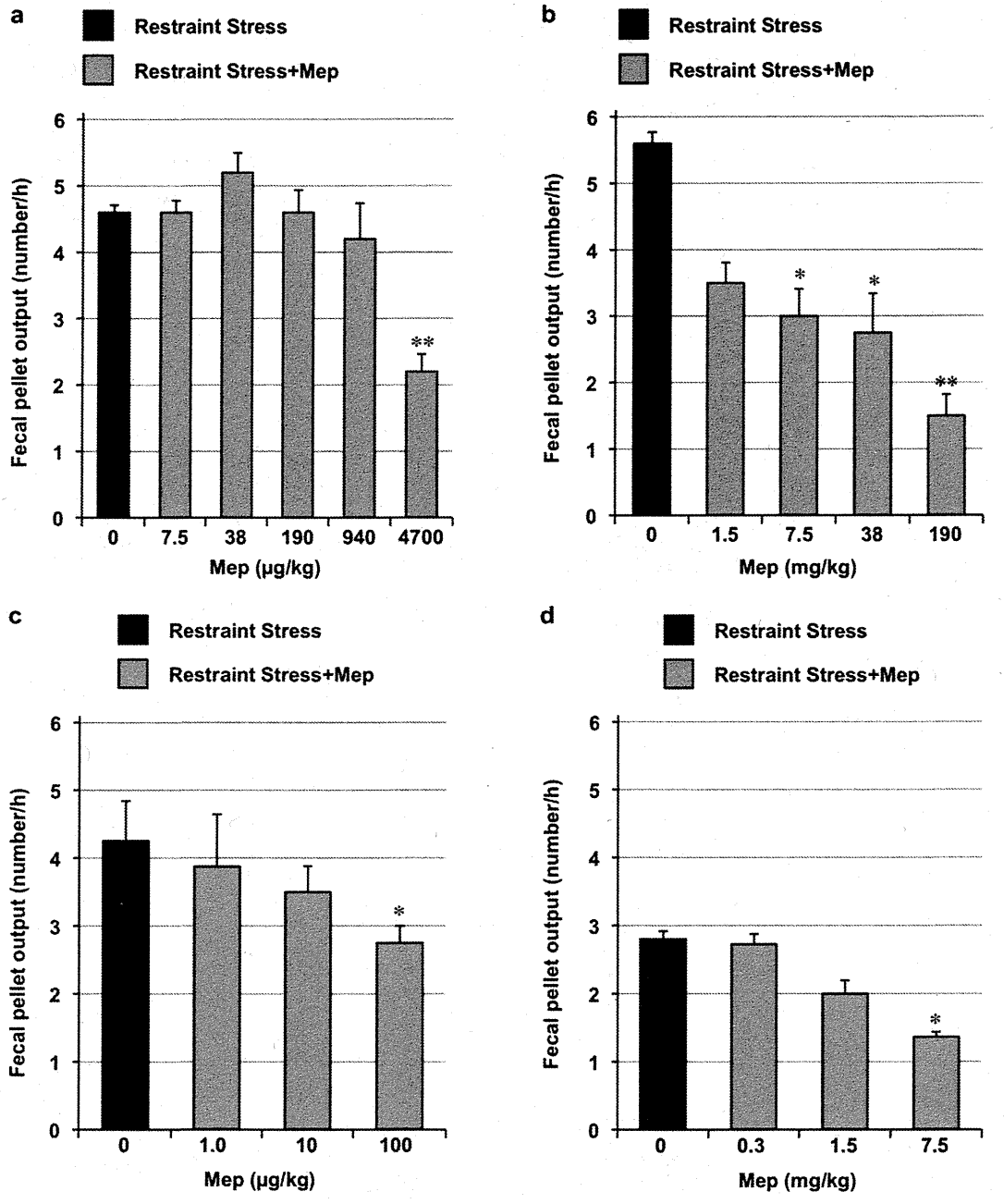

Figure 7 | Effect of mepenzolate on fecal pellet output. Mice were administered indicated doses of mepenzolate intratracheally (a), orally (b), intravenously (c) or intrarectally (d). One hour later, mice were exposed to restraint stress. The number of fecal pellets excreted during the restraint stress period (1 h) was determined. Values represent mean 6 S.E.M. (n 5 4⊠5). * P , 0.05; ** P , 0.01.

For the intravenous administration of mepenzolate, mice were maintained under anesthesia with chloral hydrate (500 mg/kg) and mepenzolate (various doses) in PBS was administered by syringe via a 26 G needle (TERUMO, Tokyo, Japan). For control mice, PBS alone was administered by the same procedure.

At day 0, the administration of mepenzolate was performed 1 h (intratracheal administration) or 0.5 h (other routes of administration) prior to the PPE administration or the CS exposure.

Preparation of BALF and cell count method. BALF was collected by cannulating the trachea and lavaging the lung with 1 ml of sterile PBS containing 50 U/ml heparin (2 times). About 1.8 ml of BALF was routinely recovered from each animal. The total cell number was counted using a hemocytometer. Cells were stained with Diff-Quik reagents after centrifugation with Cytospin㈎ 4 (Thermo Electron Corporation, Waltham, MA), and the ratio of number of neutrophils to total cell number was examined to determine the number of neutrophils.

Histopathological analysis. Lung tissue samples were fixed in 10% formalin neutral buffer solution for 24 h at a pressure of 25 cmH_2O, and then embedded in paraffin before being cut into 4 μm-thick sections. Sections were stained first with Mayer's hematoxylin and then with 1% eosin alcohol solution (H & E staining). Samples were mounted with malinol and inspected with the aid of an Olympus BX51 microscope (Tokyo, Japan).

To determine the MLI (an indicator of airspace enlargement), 20 lines (500 μm) were drawn randomly on the image of a section and intersection points with alveolar walls were counted to determine the MLI. This morphometric analysis was conducted by an investigator blinded to the study protocol.

Measurement of lung mechanics, airway resistance and $FEV_{0.05}$/FVC. Lung mechanics and airway resistance were monitored with a computer-controlled small-animal ventilator (FlexiVent, SCIREQ, Montreal, Canada), as described previously[18,19]. Mice were anesthetized with chloral hydrate (500 mg/kg), a tracheotomy was performed, and an 8 mm section of metallic tube was inserted into the trachea. Mice were mechanically ventilated at a rate of 150 breaths/min, using a tidal volume of 8.7 ml/kg and a positive end-expiratory pressure of 2–3 cmH_2O.

Total respiratory system elastance and tissue elastance were measured by the snapshot and forced oscillation techniques, respectively. All data were analysed using FlexiVent software (version 5.3; SCIREQ, Montreal, Canada).

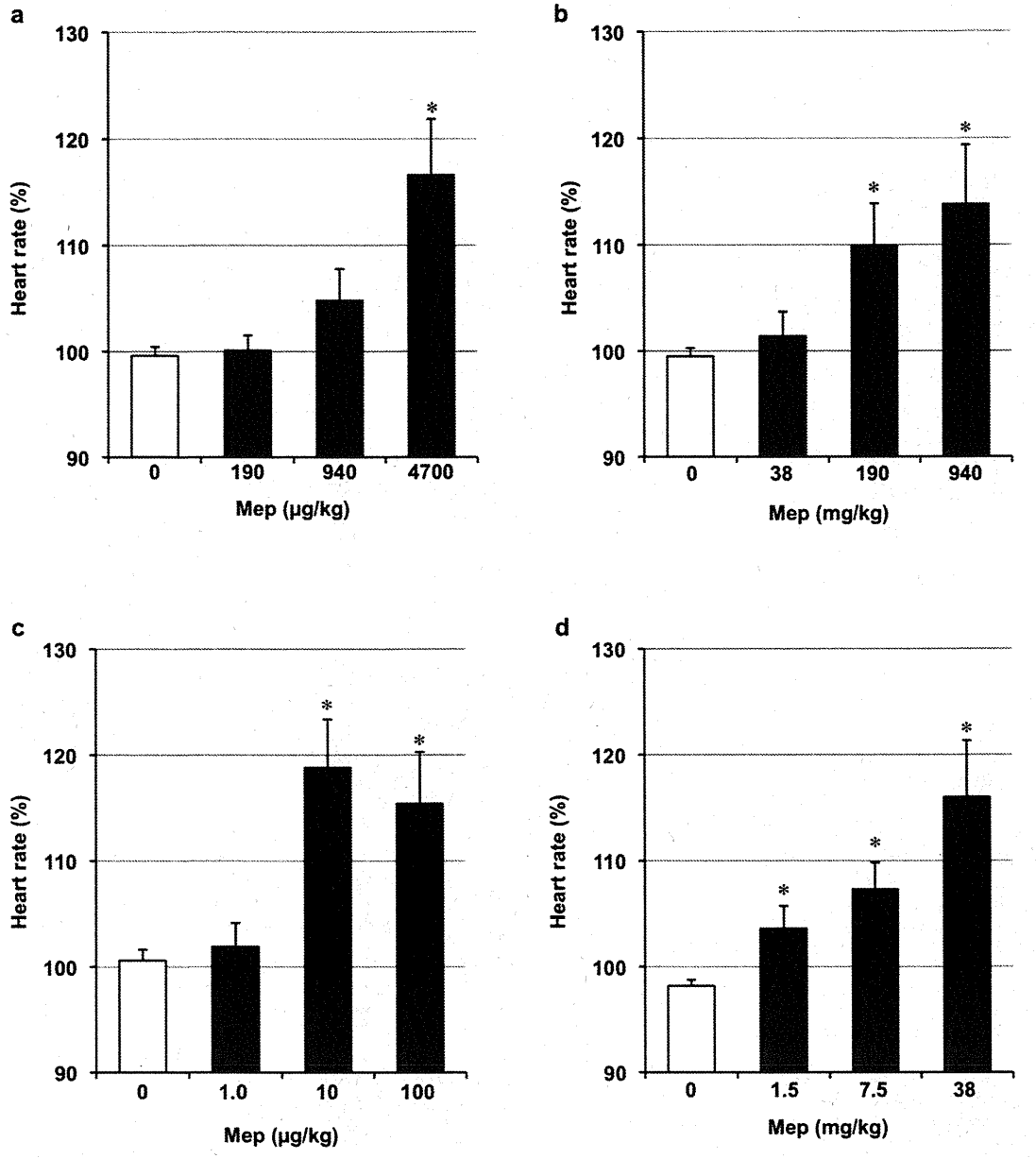

Figure 8 | Effect of mepenzolate on heart rate. Mice were administered indicated doses of mepenzolate intratracheally (a), orally (b), intravenously (c) or intrarectally (d). The alteration of heart rate (beats per minute) by the mepenzolate administration was monitored as described in the Materials and Methods. Mepenzolate-dependent alteration of heart rate from the baseline to the peak is shown. Values represent mean 6 S.E.M. (n5 3☒). * P , 0.05; ** P , 0.01.

For measurement of methacholine-induced increases in airway resistance, mice were exposed to nebulized methacholine (1 mg/ml) five times for 20 sec with a 40 sec interval, and airway resistance was measured after each methacholine challenge by the snapshot technique. All data were analysed using the FlexiVent software.

Determination of the FEV0.05/FVC (forced expiratory volume in the first 0.05 seconds to forced vital capacity) ratio was performed with the same computer-controlled small-animal ventilator connected to a negative pressure reservoir (SCIREQ, Montreal, Canada), as described previously[18,19]. Mice were tracheotomised and ventilated as described above. The lung was inflated to 30 cmH_2O over one second and held at this pressure. After 0.2 sec, the pinch valve (connected to ventilator) was closed and after 0.3 sec, the shutter valve (connected to negative pressure reservoir) was opened for exposure of the lung to the negative pressure. The negative pressure was held for 1.5 sec to ensure complete expiration. FEV0.05/FVC was determined using the FlexiVent software.

Table 1 | Efficacy versus toxicity ratio for different routes of mepenzolate administration

Administration route	Intratracheal	Oral	Intravenous	Intrarectal
Efficacy	38 μg/kg	190 mg/kg	10 μg/kg	1.5 mg/kg
Toxicity	4700 μg/kg	7.5 mg/kg	10 μg/kg	1.5 mg/kg
Toxicity/Efficacy	120	0.04	1	1

The effective dose (efficacy) was determined as the minimum dose required to significantly suppress the PPE-induced increase in MLI (Figs. 1c, 2c, 3c and 5c). The toxic dose (toxicity) was determined as the minimum dose required to significantly affect either fecal pellet output or heart rate (Figs. 7 and 8). The ratio of the toxic dose versus the effective dose for each route of administration is shown.

Analysis of fecal pellet output. Mice were subjected to restraint stress by being placed individually into a 50 ml tube (Becton Dickinson, Franklin Lakes, NJ) for 1 h, as described previously[28]. These tubes are small enough to restrain a mouse so that it is able to breathe but unable to move freely. The number of fecal pellets excreted during the restraint stress period (1 h) was measured.

Measurement of heart rate. Heart rate was measured with a MouseOx system (STARR Life Sciences Corp., Allison Park, PA), as described previously[29]. Mice were anesthetized with chloral hydrate (500 mg/kg) and the sensor was attached to the thigh. Heart rate was determined using MouseOx software (STARR Life Sciences Corp., Allison Park, PA).

Determination of the level of mepenzolate in vivo. After administration of mepenzolate, blood samples (800 μl) were taken periodically into centrifuge tubes containing heparin (50 μl) and centrifuged immediately (1000 3 g, 10 min) to obtain the sample. Whole lungs were taken from mepenzolate-treated mice, homogenised in sterile PBS containing 50 U/ml heparin, and centrifuged (14, 000 3 g, 1 min) to obtain the sample. An aliquot (300 μl) of each sample was ultrafiltered with an Amicon utra-0.5 centrifugal filter to extract the mepenzolate. The filtrate was analysed by analytical HPLC with a reverse-phase column (TSKgel Super-ODS, 150 3 4.6 mm, 2 μm, Tosoh Co., Tokyo, Japan), Waters 2695 Alliance separation module, and a Waters 2996 photodiode array detector (Waters, Milford, MA). Solution containing 30% (v/v) acetonitrile and 14 mM potassium dihydrogen phosphate/sodium 1-propanesulfonate buffer was used at a flow rate of 0.3 ml/min. Detection was performed at an optical density of 220 nm.

Statistical analysis. All values are expressed as the mean 6 S.E.M. Two-way ANOVA followed by the Tukey test or the Student's t-test for unpaired results was used to evaluate differences between three or more groups or between two groups, respectively. Differences were considered to be significant for values of P , 0.05.

1. Rabe, K. F. et al. Global strategy for the diagnosis, management, and prevention of chronic obstructive pulmonary disease: GOLD executive summary. Am J Respir Crit Care Med **176**, 532–555 (2007).
2. Barnes, P. J. & Stockley, R. A. COPD: current therapeutic interventions and future approaches. Eur Respir J **25**, 1084–1106 (2005).
3. Owen, C. A. Proteinases and oxidants as targets in the treatment of chronic obstructive pulmonary disease. Proc Am Thorac Soc **2**, 373–385; discussion 394–375 (2005).
4. Tashkin, D. P. et al. A 4-year trial of tiotropium in chronic obstructive pulmonary disease. N Engl J Med **359**, 1543–1554 (2008).
5. Calverley, P. M. et al. Salmeterol and fluticasone propionate and survival in chronic obstructive pulmonary disease. N Engl J Med **356**, 775–789 (2007).
6. Alsaeedi, A., Sin, D. D. & McAlister, F. A. The effects of inhaled corticosteroids in chronic obstructive pulmonary disease: a systematic review of randomized placebo-controlled trials. Am J Med **113**, 59–65 (2002).
7. Barnes, P. J., Ito, K. & Adcock, I. M. Corticosteroid resistance in chronic obstructive pulmonary disease: inactivation of histone deacetylase. Lancet **363**, 731–733 (2004).
8. Mizushima, T. Drug discovery and development focusing on existing medicines: drug re-profiling strategy. J Biochem **149**, 499–505 (2011).
9. Tanaka, K. et al. Mepenzolate bromide displays beneficial effects in a mouse model of chronic obstructive pulmonary disease. Nat Commun **4**, (2013).
10. Chen, J. Y. Antispasmodic activity of JB-340 (N-methyl-3-piperidyl-diphenylglycolate methobromide) with special reference to its relative selective action on the sphincter of Oddi, colon and urinary bladder of the dog. Arch Int Pharmacodyn Ther **121**, 78–84 (1959).
11. Buckley, J. P., De, F. J. & Reif, E. C. The comparative antispasmodic activity of N-methyl-3-piperidyl diphenylglycolate methobromide (JB-340) and atropine sulfate. J Am Pharm Assoc Am Pharm Assoc (Baltim) **46**, 592–594 (1957).
12. Long, J. P. & Keasling, H. H. The comparative anticholinergic activity of a series of derivatives of 3-hydroxy piperidine. J Am Pharm Assoc Am Pharm Assoc (Baltim) **43**, 616–619 (1954).
13. Drummond, G. R., Selemidis, S., Griendling, K. K. & Sobey, C. G. Combating oxidative stress in vascular disease: NADPH oxidases as therapeutic targets. Nat Rev Drug Discov **10**, 453–471 (2011).
14. Gosker, H. R. et al. Altered antioxidant status in peripheral skeletal muscle of patients with COPD. Respir Med **99**, 118–125 (2005).
15. Rahman, I. & MacNee, W. Antioxidant pharmacological therapies for COPD. Curr Opin Pharmacol **12**, 256–265 (2012).
16. Prat, M., Gavalda, A., Fonquerna, S. & Miralpeix, M. Inhaled muscarinic antagonists for respiratory diseases: a review of patents and current developments (2006–2010). Expert Opin Ther Pat **21**, 1543–1573 (2011).
17. Kuraki, T., Ishibashi, M., Takayama, M., Shiraishi, M. & Yoshida, M. A novel oral neutrophil elastase inhibitor (ONO-6818) inhibits human neutrophil elastase-induced emphysema in rats. Am J Respir Crit Care Med **166**, 496–500 (2002).
18. Tanaka, K. et al. Therapeutic effect of lecithinized superoxide dismutase on pulmonary emphysema. J Pharmacol Exp Ther **338**, 810–818 (2011).
19. Tanaka, K., Sato, K., Aoshiba, K., Azuma, A. & Mizushima, T. Superiority of PC-SOD to other anti-COPD drugs for elastase-induced emphysema and alteration in lung mechanics and respiratory function in mice. Am J Physiol Lung Cell Mol Physiol **302**, L1250–1261 (2012).
20. Bergogne-Berezin, E. & Bryskier, A. The suppository form of antibiotic administration: pharmacokinetics and clinical application. J Antimicrob Chemother **43**, 177–185 (1999).
21. Sasaki, K., Yonebayashi, S., Yoshida, M., Shimizu, K., Aotsuka, T. & Takayama, K. Improvement in the bioavailability of poorly absorbed glycyrrhizin via various non-vascular administration routes in rats. Int J Pharm **265**, 95–102 (2003).
22. Agarwal, R. & Jindal, S. K. Acute exacerbation of idiopathic pulmonary fibrosis: a systematic review. Eur J Intern Med **19**, 227–235 (2008).
23. Verhamme, K. M. et al. Tiotropium Handihaler and the risk of cardio- or cerebrovascular events and mortality in patients with COPD. Pulm Pharmacol Ther **25**, 19–26 (2012).
24. Gross, N. J., Giembycz, M. A. & Rennard, S. I. Treatment of chronic obstructive pulmonary disease with roflumilast, a new phosphodiesterase 4 inhibitor. COPD **7**, 141–153 (2010).
25. Miravitlles, M. & Anzueto, A. Insights into interventions in managing COPD patients: lessons from the TORCH and UPLIFT studies. Int J Chron Obstruct Pulmon Dis **4**, 185–201 (2009).
26. Rajendrasozhan, S., Yang, S. R., Edirisinghe, I., Yao, H., Adenuga, D. & Rahman, I. Deacetylases and NF-kappaB in redox regulation of cigarette smoke-induced lung inflammation: epigenetics in pathogenesis of COPD. Antioxid Redox Signal **10**, 799–811 (2008).
27. Ito, K. et al. Histone deacetylase 2-mediated deacetylation of the glucocorticoid receptor enables NF-kappaB suppression. J Exp Med **203**, 7–13 (2006).
28. Asano, T. et al. Effects of beta-(1,3-1,6)-D-glucan on irritable bowel syndrome-related colonic hypersensitivity. Biochem Biophys Res Commun **420**, 444–449 (2012).
29. McLaughlin, B., Buendia, M. A., Saborido, T. P., Palubinsky, A. M., Stankowski, J. N. & Stanwood, G. D. Haploinsufficiency of the E3 ubiquitin ligase C-terminus of heat shock cognate 70 interacting protein (CHIP) produces specific behavioral impairments. PLoS One **7**, e36340 (2012).

Acknowledgments

We thank Dr. Tomoko Betsuyaku (Keio University) for helpful discussion and Mrs. Kumi Matsuura (Kumamoto University) for technical assistance. This work was supported by Grants-in-Aid for Scientific Research from the Ministry of Health, Labour, and Welfare of Japan, as well as the Japan Science and Technology Agency and Grants-in-Aid for Scientific Research from the Ministry of Education, Culture, Sports, Science and Technology, Japan.

Author contributions

Conception and design: K.T. and T.M.; Analysis and interpretation: K.T., T.A., N.Y., D.K., Y.Y., H.Y., S.K. and T.I.; Drafting the manuscript for important intellectual content: K.T., T.A., N.Y., H.W., T.M., H.S. and T.M.

Additional information

Competing financial interests: The authors declare no competing financial interests.

How to cite this article: Tanaka, K.-I. et al. Superiority of pulmonary administration of mepenzolate bromide over other routes as treatment for chronic obstructive pulmonary disease. Sci. Rep. **4**, 4510; DOI:10.1038/srep04510 (2014).